Development of a Micropatterned ZSM-5 Model System

Guido de Reijer

Daily supervisors : Koen Bossers MSc & Laurens Mandemaker MSc

First examiner: Prof. Dr. Ir. Bert Weckhuysen

Second examiner: Dr. Florian Meirer

Inorganic Chemistry and Catalysis

Faculty of Science

Debye Institute for Nanomaterials Science

Abstract

In order to design and fabricate a planar zeolite model system which can be used for high-throughput screening of catalytic tests, the development of a micropatterned ZSM-5 thin film has been explored. Several techniques have been investigated including the spin-coating of an acidic colloidal solution followed by hydrothermal synthesis of SBA-15 and recrystallization to ZSM-5, direct-dipping hydrothermal synthesis of silicalite-1 & ZSM-5, spin-coating of alkaline and neutral solutions followed by steam-assisted crystallization into silicalite-1 & ZSM-5 and microinjection followed by steam-assisted crystallization into silicalite-1. Synthesized model systems have been analysed with optical microscopy, scanning electron microscopy, atomic force microscopy and X-ray diffraction. Direct-dipping hydrothermal synthesis has led to a micropatterned MFI zeolite thin film model system and microinjection has led to the highest control over the composition of zeolite micropatterns.

Content

Chapter 1 – Introduction

In modern day society, the rapid expansion and development of the human race is requiring more resources every day.[1] This increased energy consumption has put extra pressure on the energy generation which is still heavily provided by burning of depleting fossil fuels.[2] This upcoming necessity for energy production combined with the increasing realization of the importance of reducing global emission of greenhouse gasses, has concentrated attention towards developing renewable energy sources as well as improving existing processes.[3]

1.1 Catalysis

One of the essential components in almost all industrial processes is the catalyst. Catalysis is a process used in both biological and industrial chemical reactions and is known to increase the reaction rate by lowering the activation energy.[4] This is achieved by offering an alternative reaction pathway of lower energy. Since catalysts are usually not consumed during their reaction but rather regenerated and able to catalyse another cycle, only little quantities can be used. There are different types of catalysts which can generally be divided in two classes: homogeneous catalysts and heterogeneous catalyst.[5] Homogeneous catalysts operate in the same reaction phase as the reagents and products whereas heterogeneous catalysts occupy a different phase. Heterogeneous catalysis often operate in solid phase while the reactants are liquid or vapour. One class of heterogeneous catalysts which is often used in many industrial processes such as cracking and processing crude oil is named zeolites.

Figure 1: Commercial zeolite pellets with spherical and cylindrical shapes. [6]

1.1.1 Zeolites

Zeolites are a group of microporous minerals that mainly consist of silicon, aluminium, oxygen and a wide variety of cations. These materials consist of distinct building blocks combined and aligned in arrays creating unique morphologies. The primary building units (PBU) of zeolites are the silica tetrahedra ($SiO_{4/2}$) and alumina tetrahedra ($AlO_{4/2}$). Bridging of PBU by oxygen atoms forms the secondary build units (SBA) which can in turn be combined and linked by oxygen to form the different zeolite framework types.[7]

Zeolites are solid catalysts that possess a high internal surface area due to the microporous framework, typically ranging from 500 to 800 m^2/g.[8] This high surface area allows for a high quantity of gases or liquids to chemisorb onto its surface and subsequently undergo reaction. An important feature of zeolites is their microporosity which gives them a high selectivity towards a number of reactions for several reasons. Firstly, zeolites operate as molecular sieves and selectively sort molecules based on their size and shape. By allowing certain reagents to enter their porous structure, allowing certain products to leave or allowing particular transition-states to form, zeolites are able to catalyse reactions with high selectivity and efficiency. [9,10] Additionally, zeolites can be used to adsorb or filter cations in aqueous systems. This selectivity is based on the distribution and amount of negative charge density in the zeolite framework. [11]

Besides, their robust stability under harsh conditions makes them perfect candidates for industrial processes.[12] A downside of their rigid, regular structure of molecular dimensions is that large molecules formed inside the pores might not be able to leave the zeolite which leads to clogging of the pores and rendering it inactive. This problem is referred to as coke formation and can be solved by burning off the formed organic species and thus regenerating the zeolite. Regeneration of the zeolite is an important part of the fluid catalytic cracking process (FCC); a process in which high-molecular weight crude oil fractions are converted into lighter, petroleum hydrocarbons. [13]

1.1.2 Zeolite Socony Mobile-5

One kind of zeolite which has received a lot of scientific interest due to its many applications is the Zeolite Socony Mobile-5, ZSM-5, which has been patented in 1975 by Mobil Oil company. ZSM-5 is a synthetic zeolite which possesses the MFI framework, referring to its name. Similar to other zeolites, its primary structural unit is a neutral silica or negatively charged alumina tetrahedron, as shown in figure 2. These tetrahedra combine to form pentasil units which are connected by oxygen bridges to form pentasil chains. On each of the intersection points of the pentasil unit there is either a silicon or aluminium cation. Likewise, these chains are interconnected by oxygen bridges forming sheets with 10-ring holes, creating straight, parallel 10-ring channels. Perpendicular to these sheets, 10-ring sinusoidal channels are formed. Both channels as well as the intersection cavity between them play a role in catalysis and adsorption. [14]

One widely researched process is the methanol-to-olefins process in which ZSM-5 is used to catalyse the conversion of green fuels into hydrocarbons.

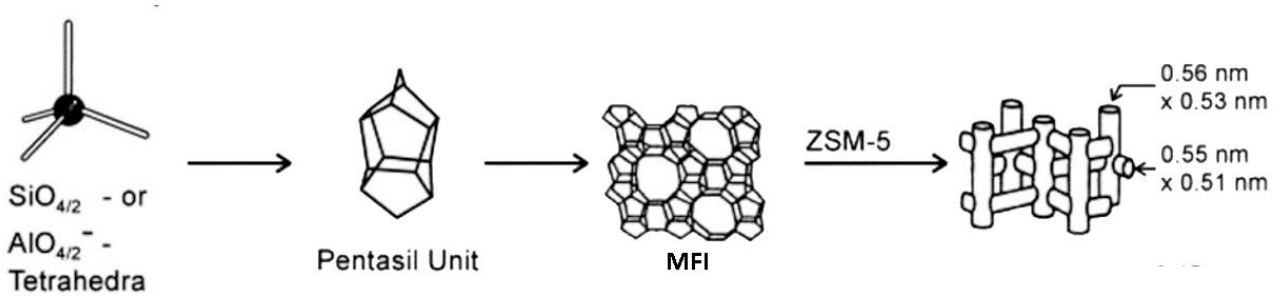

Figure 2: Schematic representation of different building blocks of zeolite ZSM-5 [14]

1.2 Model system

Fundamental research is required to fully understand the chemistry behind catalysts down to the (sub)-nanometre regime. Not only is this research essential to develop catalysts with higher activity but also to reduce waste, costs and its negative impact on the environment. One important tool which is used in this field of research and understanding the chemistry at molecular level is through the use of model systems.

These model systems can simplify, approximate or investigate natural phenomena or existing scientific models. In chemistry and in particular in catalysis, model systems can range from describing the riser and regenerator reactors of the aforementioned industrial FCC units [15] to single crystal analysis or even smaller investigating nanoparticle clusters.[16]

1.2.1 Thin film model system

One model system which has shown promising applications is the thin film model. In zeolite thin films, chemical processes such as diffusion or catalysis inside single zeolite channels can be studied. Through control of zeolite growth stage during the synthesis, highly oriented zeolite films such as b-oriented ZSM-5 films can be synthesized with accessibility to only straight zeolite channels.[17] Studies investigating the catalytic mechanism in single pore orientation zeolite films can be compared to bulk studies leading to chemical understanding on a molecular level. Additionally, thin films can be investigated using more sophisticated and advanced characterization techniques, as opposed to bulk catalyst or supported catalyst particles. Examples of these techniques include atomic force microscope infrared-microscopy (AFM-IR) [18], tip-enhanced Raman spectroscopy (TERS)[19], grazing incidence characterization techniques like grazing incidence X-ray diffraction (GI-XRD)[20] or photoinduced force microscopy enabling nanoscale infrared imaging of e.g. ZSM-5. [21]

Similar to zeolites in powder form, zeolite films exhibit excellent thermal, mechanical and thermal stability as well as a unique pore morphology.[22] Moreover, thin film models are used to design thin films which can be applied in electrochemistry, as a coating or in separation processes.[23] For example as a membrane in the separation of oil and water, which has become an increasingly important issue with the upcoming interest in environmental protection.[24]

An important feature of a high quality thin film is its high uniformity of thickness and composition of the film. However, this well-ordered homogeneity does not allow for variety within a model system and that is why the micropatterned film model system has been explored.

1.2.2 Micropatterned film model system

The micropatterned model system is similar to the thin film model since a thin layer of material is attached onto a substrate but instead of one homogenous layer covering the entirety of the substrate, microscopically small, separate areas of zeolite material are attached to the substrate (figure 3). The major advantage of these separate 'islands' of material is the ability to alter the composition of areas or distinct islands. Besides, if the wettability of the zeolite is controlled and tuneable, hemispherical zeolite particles can be synthesized simulating particle morphology in industry. [25]

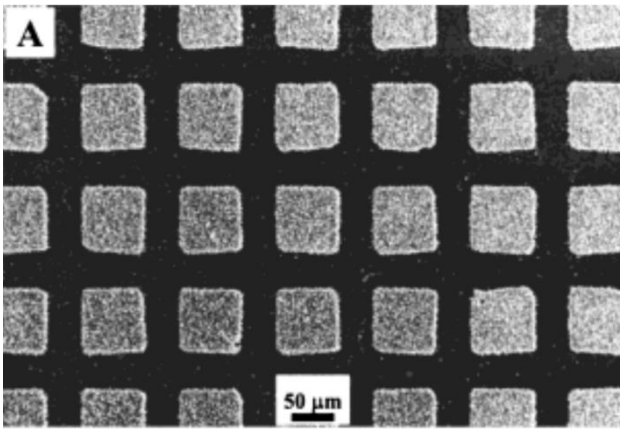

Figure 3: SEM image of micropatterned zeolite on glass [26]

This enables several promising experiments such as high-throughput screening (HTS); an important technique in modern drug discovery research.[27] HTS assays enable testing of a large amount of samples or analytes for chemical substances in one screening, usually with the help of robotics. In the field of catalysis, HTS can be applied when using a fluorescence-based assay in which successful binding of organic molecules leads to a visibly colour chance indicating catalytic activity or potential. [28]

High throughput screening of catalytic tests will require a high-throughput synthesis of micropatterned zeolite films to unlock the full potential of the model system. One possible method is the use of printing of zeolite material, such as H-ZSM-5, onto a substrate.[29] For the micropatterning, an inkjet printer which uses zeolite as filler can be applied and different areas with different zeolite precursor solution can be applied onto the same substrate. This allows for promising comparative studies in which one substrate is micropatterned with zeolite areas of different composition and takes place in an e.g. catalytic reaction. All reaction conditions and parameters remain constant except for one parameter which is subject to being tested. This micropatterned thin film model system offers a promising application compared with the thin film model system. Liu et al. have designed a high-throughput generation of mesoporous metal oxides libraries using inkjet

printing (figure 4).[30] Colloidal nanoparticles ink (A) is used for printing followed by fast catalyst exploration (B).

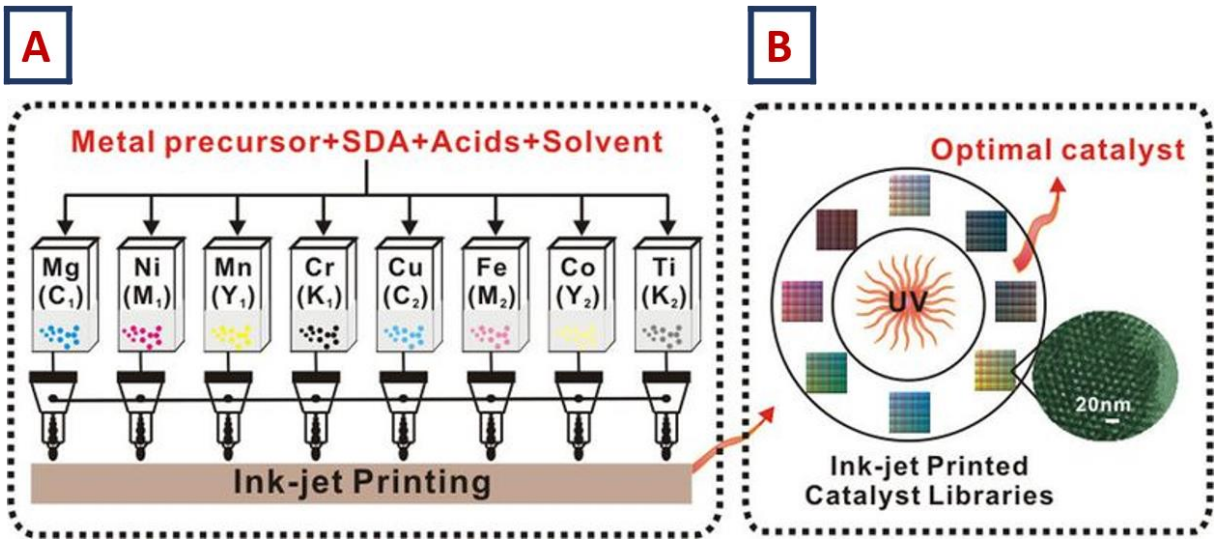

Figure 4: Schematic representation of inkjet printing used to fabricate catalyst libraries [30]

1.3 Research aim

In order to explore these promising applications, the fabrication of such a model system needs to be realised. There is a number of important factors to take into account such as the choice of the substrate and the role of the substrate itself during the growth of a zeolite micropatterned film. Moreover, the crystal growth of ZSM-5 itself needs to be understood and controlled so that a micropatterned model system is fabricated instead of a thin film model system. Finally, the different methods of altering the composition of separate areas of zeolite material must be explored.

These aims can be combined into the research aim of this study which is the following:

To develop an understanding of the formation processes during the synthesis of a ZSM-5 micropatterned model system.

Chapter 2 - Theory

In this research, several approaches to synthesize a micropatterned zeolite model system have been explored. These approaches involve a number of chemical and physical processes important to either the zeolite synthesis or substrate preparation, which are discussed below.

2.1 Zeolite acidity

As mentioned in section 1.1.2, the primary building units of zeolite ZSM-5 consist of silica and alumina tetrahedra (figure 5). These tetrahedra consist of silicon (Si^{4+}) or aluminium (Al^{3+}) tetrahedrally bonded to four oxygen (O^{2-}) ions. Since each framework oxygen is bond to two framework metals, the charge is shared resulting in the molecular formula of neutral $[SiO_{4/2}]^0 = SiO_2$ and negatively charged $[AlO_{4/2}]^- = [AlO_2]^-$ for the silica and alumina tetrahedra, respectively. [31]

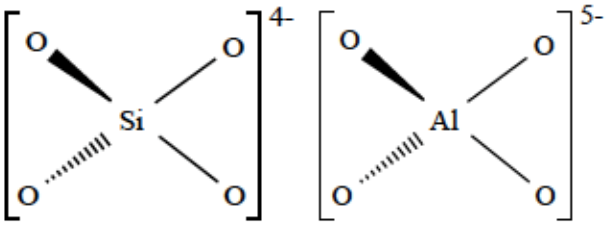

Figure 5: Silica and alumina tetrahedra[31]

In both natural and synthetic silicate minerals, the silica tetrahedra are linked together through sharing an oxygen ion resulting in a variety of arrangements (figure 6).

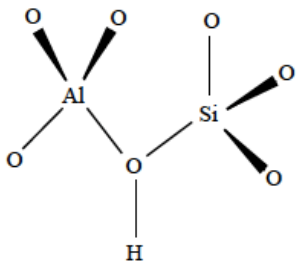

Figure 6: Tetrahedral arrangement of Si-O & Al-O bonding [31]

Since the alumina tetrahedron possesses a different charge than the silica tetrahedron, substitution of silica by alumina results in a net negative charge on the zeolite framework which needs to be compensated by extra-framework cations. This substitution gives rise to Brønsted acidity since protons can act as these cations which in turn can participate in acid-catalytic reactions such as methanol-to-hydrocarbons (figure 7).

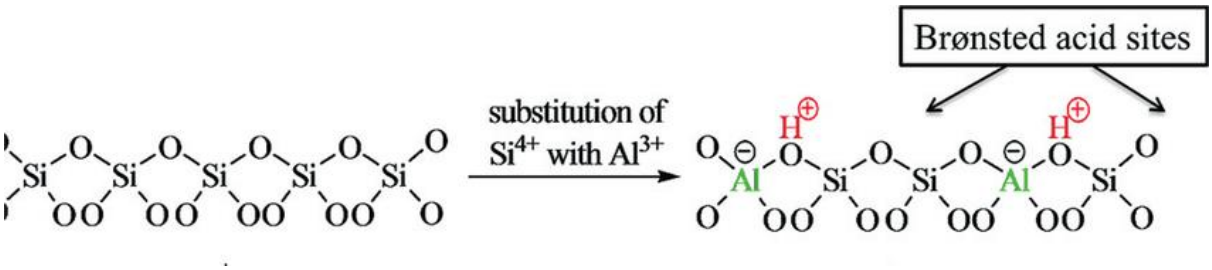

Figure 7: Schematic formation of a Brønsted acid site by Si/Al substitution and a proton counter ion [32]

The strength of these Brønsted acid sites depends on the next-nearest neighbour aluminium, it decreases with other nearby Brønsted acid sites. This is influenced by framework aluminium ions and thus the Si/Al ratio of the zeolite. The increased local population of protons weakens the acidity of each individual acid site while the total zeolite acidity increases.

Lewis acidity may also be present due to aluminium present outside the framework of the zeolite; for example as alumina dispersed in the pore structure or on the exterior of the zeolite crystal. Nonetheless, zeolite have Lewis acid site that are generally weaker than their Brønsted acid sites. [33]

2.2 Zeolite nucleation & crystal growth

The synthesis of zeolites is based on two processes which occur both simultaneously & sequentially: nucleation & growth.

Nucleation of zeolites is defined as the formation of a crystal from a solution or in a vapour. This is often accompanied by supersaturation of its building blocks (homogeneous) or catalysed by addition of external material (heterogeneous, seeding). Usually, as is the case for ZSM-5, nucleation is preceded by growth of amorphous precursor particles which are converted into crystalline material.[34] Even though zeolite crystallization can also be initiated by conversion of colloidal suspensions (section 2.2.1)[35]

Subsequent growth processes involve assimilation of monomers from the solution.[36] In addition, agglomeration of nanoparticles with crystal surfaces can also lead to chemical bonding. [37]

2.2.1 Sol-gel process

One method of converting small, silica containing molecules into large, periodically organized zeolite materials involves the sol-gel process.[38] This technique consists of several steps starting with the hydrolysis and polycondensation of organometallic precursors such as silicon alkoxides [$Si(OR)_3$]. Initial rapid hydrolysis leads to the formation of a colloidal solution, 'sol', in which both solid phase and liquid phase precursor particles are present. Simultaneous polycondensation of hydrolysed species leads to the formation of an interconnected 3-D network resulting in a silica gel consisting of bond silicon alkoxides. Subsequent gelation and drying leads to the final amorphous compound which can be crystallized into zeolites.

The initial hydrolysis step occurs through formation of a penta-coordinated intermediate. This reaction can be catalysed both by acid (pH<2) or base. Under acidic conditions (figure

8), initial protonation of the silica alkoxides withdraws electron density from the silicon atom, making it more susceptible to attack by nucleophilic water. After attack by water from the rear, a transition state of S_N2-type character is created resulting in the decreased positive charge on the protonated alkoxide and subsequent release of the alcohol. [39,40]

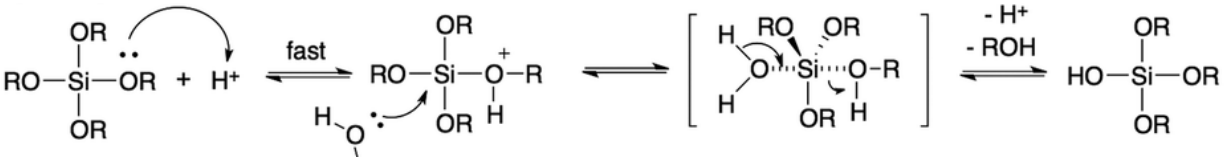

Figure 8: Schematic diagram of hydrolysis of a silicon alkoxide.[39] Where R is an alkyl chain.

Under alkaline conditions (figure 9), nucleophilic attack of hydroxide ions on the rear of the silicon atom leads to a transition state of S_N2-type character followed by the release of the alcohol. Under basic conditions, hydrolysis is the rate-determining step while under acidic conditions, condensation is the rate-determining step.

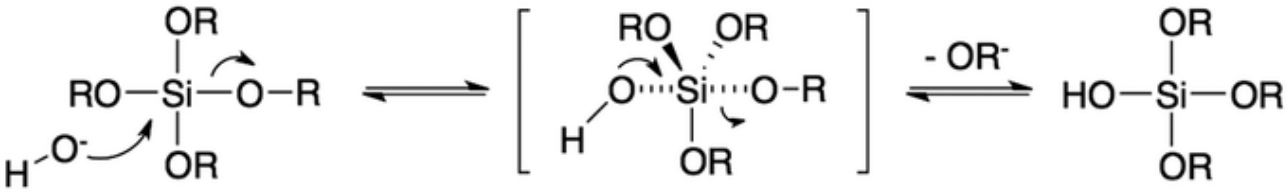

Figure 9: Schematic diagram of hydrolysis of a silicon alkoxide under alkaline conditions.[39] Where R is an alkyl chain.

Hydrolysis is quickly followed by condensation resulting in the formation of a gel network silicon alkoxides bond by siloxane bonds (Si-O-Si). Condensation takes place by either alcohol or water elimination and can both be acid catalysed (figure 10) or base catalysed (figure 11).

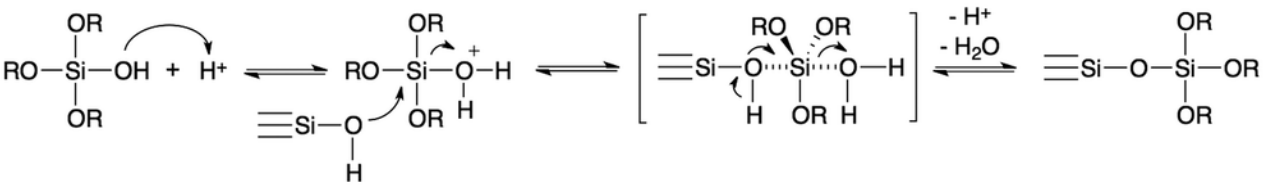

Figure 10: Schematic diagram of condensation of a silicon alkoxide under acidic conditions.[39]

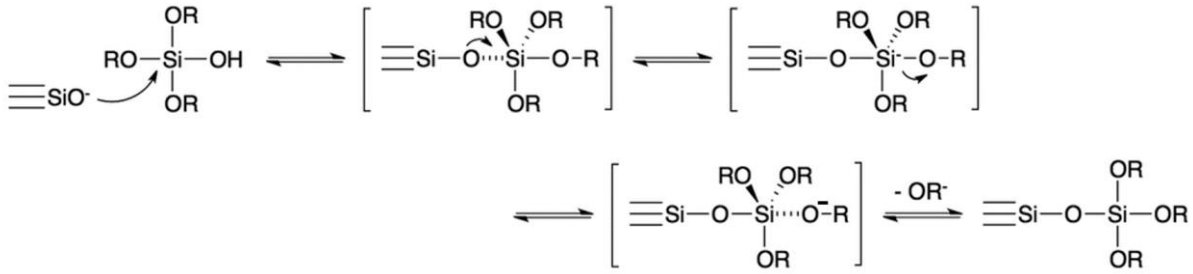

Figure 11: Schematic diagram of condensation of a silicon alkoxide under alkaline conditions.[39] Where R is an alkyl chain.

Both acid and base catalysed hydrolysis and condensation are used in the synthesis of siliceous materials and zeolites and each result in specific properties**.** Acid catalysed hydrolysis and condensation generally leads to a low degree of interconnection in the 3D silica network results in the formation of microporous structures. A potential explanation for this is the high rate of hydrolysis compared to condensation.

In base catalysed hydrolysis and condensation, larger uniform silica particles are formed leading to a broader distribution of large pores.[41] The pore dimensions and distribution can be readily tailored by introducing an organic surfactant as structure directing agent (SDA) into the colloidal solution enabling synthesis of both microporous and mesoporous structures. Factors such as the type of SDA, supplementary chemicals and synthesis conditions play a role in tuning the morphology. [42]

2.2.2 SBA-15 synthesis

An example of using an organic SDA to synthesize mesoporous silica using the sol-gel process is the synthesis of zeolite Santa Barbara Amorphous-15 (SBA-15). Among all mesoporous silica materials, SBA-15 is the most intensively studied because of its remarkable characteristics like its high surface area and pore volume, high thermal stability and straight cylindrical pores rendering it as a promising zeolite or support material. [43] In the synthesis of SBA-15, a triblock copolymer named pluronic P123 (M ≈ 5800 g/mol) is used to obtain the hexagonal morphology. In acidic medium (pH ≈1), P123 molecules exist as micelles which interact with protonated silicate species originating from dissolved tetraethyl orthosilicate (TEOS). This interaction leads to cooperative supramolecular self-assembly which results in a 2-D array of long 1-D cylindrical pores. After calcination, the template is burned off and a mesoporous silicate zeolite is formed (figure 12).[44,45] SBA-15 can in turn be converted into microporous ZSM-5 through impregnation with an aqueous solution of another SDA called tetrapropylammonium hydroxide (TPAOH) and an aluminium source.[46]

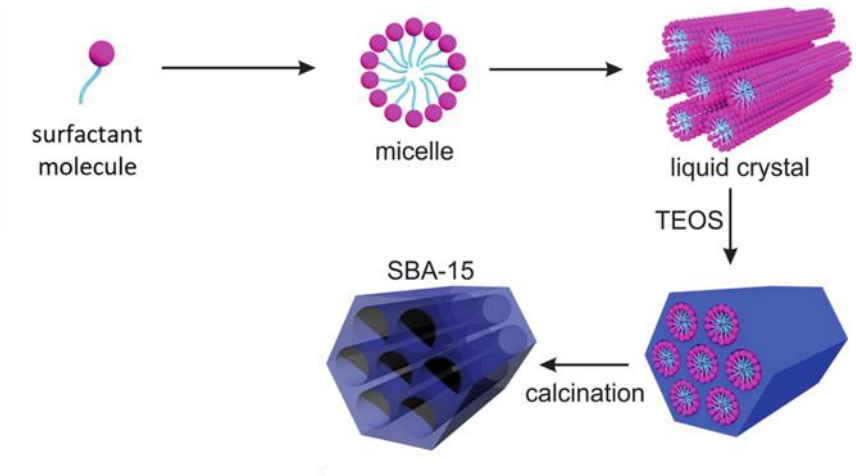

Figure 12: Schematic diagram of formation of SBA-15 using P123 as template.[45]

2.3 Substrate preparation

Silicon based substrates have found many promising applications as membranes, biological sensors, memory chips, micro- and opto-electronic devices.[47,48] However, in order to be applied in the synthesis of a model system, the substrate needs to be cleaned and prepared accordingly. Moreover, the substrate needs to be susceptible to micropatterning in order to synthesize a micropatterned thin film model.

2.3.1 Micropatterning

Under ambient conditions, elemental silicon is not inert but rather reacts with oxygen present in air to form silica, in a similar manner to many other metals and metalloids. However, the growth of this native silica layer is restricted to a maximum thickness of ≈ 2 nm.[49] Additionally, this hydrophobic layer of silica contains a layer of hydrophilic surface silanol groups (≡Si-OH) which act as dominant sites for analyte interactions and adsorption.[50]

The concentration of surface silanol groups and the distribution of different silanol groups is dependent on the impurities and synthesis methods of the substrate (figure 13).

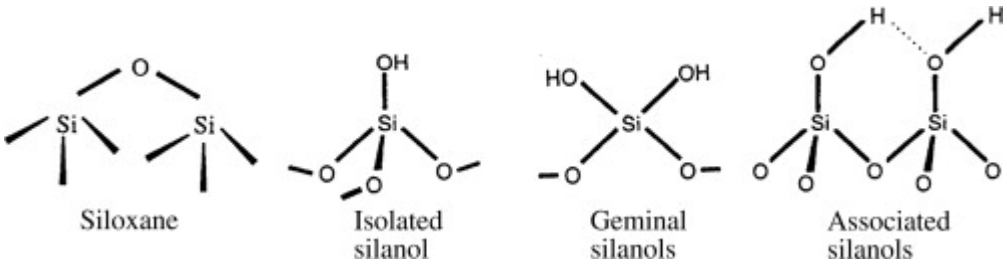

Figure 13: Schematic diagram of different silanol groups present on silicon based substrates [50]

An important characteristic of a model system is its reproducibility and surface homogeneity. Therefore, the substrate needs to be pre-treated to obtain a regular and reproducible pattern of surface groups before zeolite synthesis. This treatment consist of several cleaning steps followed by hydroxylation creating an even distribution of hydrophilic surface silanol groups which are prone to reaction with zeolite precursor solutions. After this procedure, the substrate is available for application of a thin film but not yet for application of a micropatterned thin film.

One method of preparing substrates for micropatterning involves the application of a hydrophobic organic layer onto the hydroxylated surface of Si, SiO_2 or Si_3N_4 wafers. This is realized through silanization of a CH_3-terminated alkylsilane, like octadecyl-trichlorosilane (ODTS, $C_{18}H_{37}Cl_3Si$). Silanization is based on the adsorption followed by the self-assembly and covalent binding of alkylsilanes onto the silicon based surface. As a result, a self-assembled monolayer (SAM) is formed which exhibits hydrophobic character due to its long 18 carbon backbone in the case of ODTS. Afterwards, this organic layer can be partially removed creating a pattern of hydrophobic and hydrophilic areas. [51]

Since siliceous zeolite precursors are hydrophilic in nature, they prefer bonding to the hydrophilic areas instead of the stable SAM which ultimately results in a patterned model system (figure 14). [52]

2.3.2 UV ozone treatment

One facile method of partially removing the organic ODTS chain of the monolayer attached to the Si <100> based surface is via UV ozone treatment. UV ozone treatment is used for surface cleaning and surface treatment of substrates. A low pressure mercury vapour discharge lamp creates high intensity UV light which leads to the generation of ozone from molecular oxygen present in air.[53] More specifically, a dominant emission peak at 185 nm dissociates oxygen leading to the formation of two radicals of oxygen which undergo further reaction forming ozone molecules. Simultaneously, another dominant emission peak at 254 nm excites organic contaminants and species on the surface of the substrate which increases their reactivity with ozone. Upon reaction, volatile compounds are formed which evaporate leading to near-atomically clean surfaces which means that almost all organic contaminants have been removed. By selectively protecting the substrate of the UV ozone treatment, areas coated with the hydrophobic monolayer remain untouched and a pattern is created of hydrophilic reactive silanol groups and hydrophobic ODTS carbon chains. Protection can be achieved by using a copper grid with squared or circular holes of 40 µm (figure 14, C).

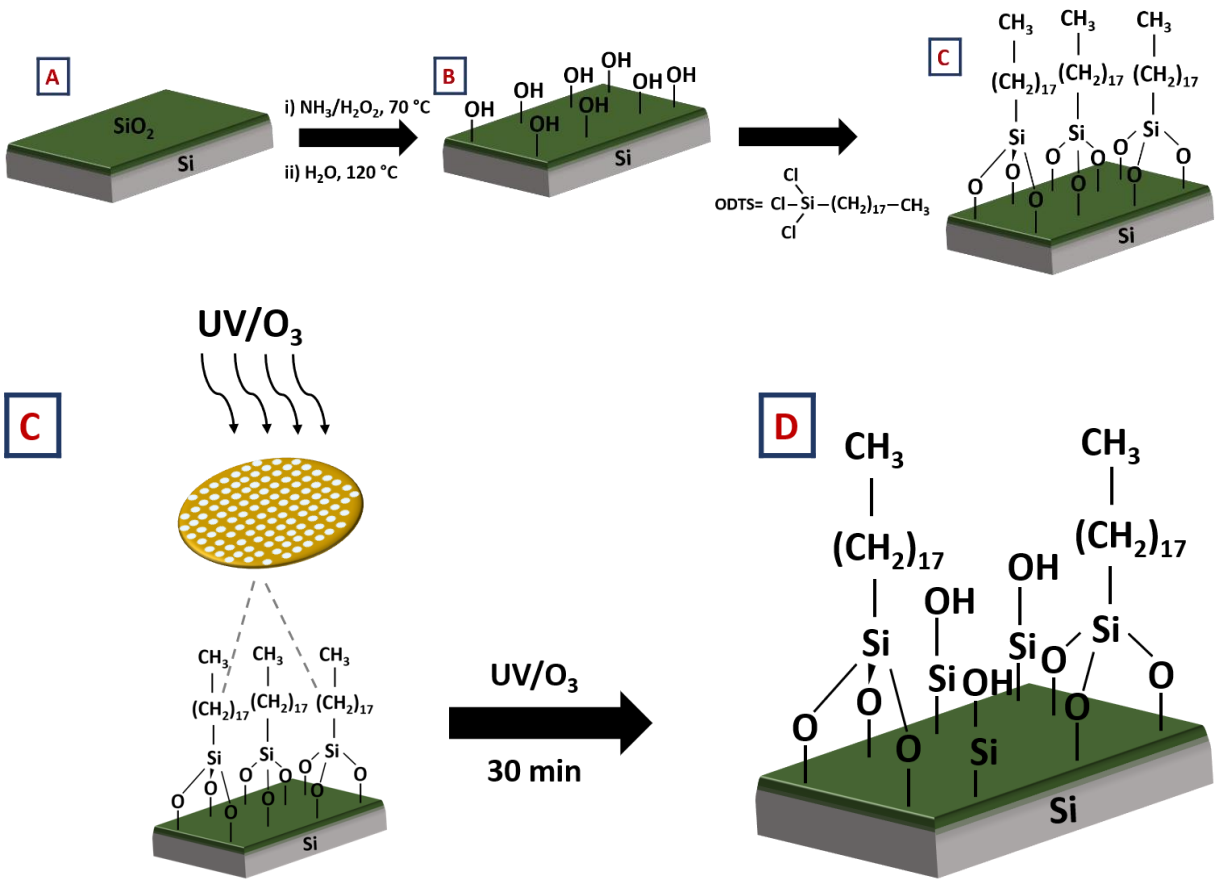

Figure 14: Schematic diagram of substrate preparation. A (coated) Si substrate is hydroxylated (a to b) followed by bonding of a hydrophobic ODTS monolayer (b to c). Micropattern of hydrophilic and hydrophobic regions is created by selectively burning organic chain using UV/ozone and a protecting copper grid.

2.3.2 Spin-coating

In the field of synthesizing thin films, a large variety of techniques have been examined, each with their own advantages and downside. For zeolite thin film synthesis based on colloidal solutions, methods include electrocoating, spray-coating, dip-coating and spin-coating.

In electrocoating, charged particles are deposited onto a conductive substrate by regulating the amount of voltage applied. It allows for the coating of structures with complex shapes, for example when used as corrosion inhibitor. [54]

In spray-coating, a sol-gel precursor solution is directly sprayed onto the substrate. Advantages of spray-coating techniques include its ability for large-area deposition and ability to spray substrates with complex shapes. [55]

Dip-coating is a convenient and easy method in which the substrate is immersed in the colloidal solution. Unfortunately, the coated layer is not always homogenous and the shape of the substrate needs to be flat in order to remove excess material through nip rolls. [56]

Another facile method is spin-coating which involves the deposition of the colloidal solution onto a spinning substrate resulting in a thin film. After deposition of the colloidal solution, the substrate is accelerated leading to radial spreading of the solution due to centrifugal force. When the substrate has reached a constant speed, the balance between the centrifugal and the friction caused by the viscosity of the solution and its affinity with the substrate leads to a homogenous spread on the substrate. Additionally, the solvent is evaporated during spinning resulting in gelation of the silica solution.[57]

The characteristics of the film can be controlled by altering the spin-coating conditions, such as the rotation speed, acceleration, duration and composition of the spin-coated solution. Generally, a higher rotation speed and duration lead to thinner films due to higher (total) centrifugal forces and longer period of solvent evaporation. Additionally, viscous solutions result in thicker films which is related to the concentration of precursors in the solution. [58] When the concentration is low, a lot of solvent is present which evaporates readily resulting in thin films. When synthesizing micro-patterned films, the affinity between the solvent and the surface groups becomes more relevant and influences the degree of spin-coating. This is the area of the substrate that consists of well defined, individual regions of precursor material (referred to as islands) with respect to the total substrate area. A substrate with a large amount of distinguishable islands is considered to have a high quality of patterning.

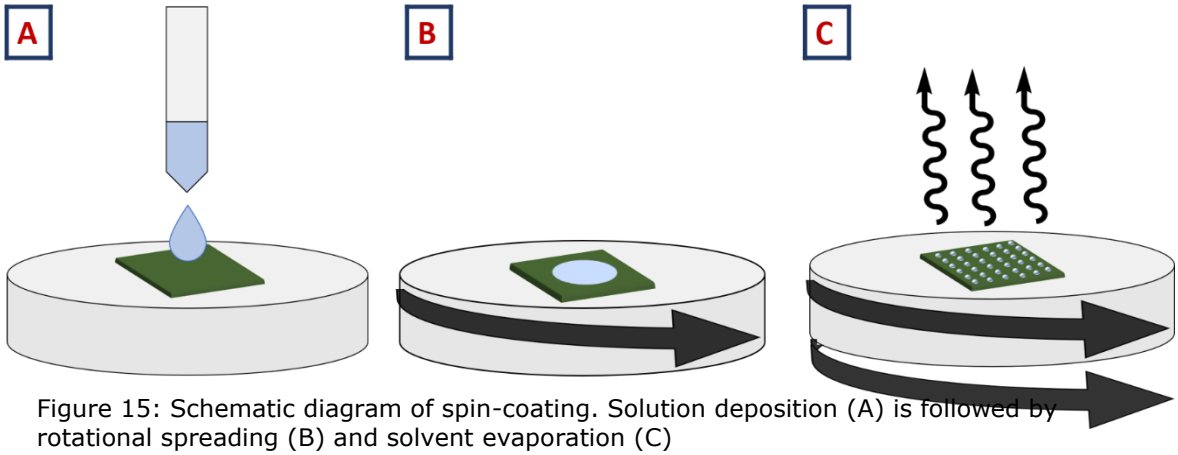

Figure 15: Schematic diagram of spin-coating. Solution deposition (A) is followed by rotational spreading (B) and solvent evaporation (C)

Chapter 3 – Experimental

During the optimization of the model system of micropatterned zeolite thin films, a variety of fabrication methods have been explored and subsequently compared. These model systems have been characterized with a number of analysis techniques.

3.1 Model synthesis

The different fabrication methods which have been explored, exhibit similarities and differences amongst each other. On the one hand, all methods use similar substrate preparation and transformation of the as-synthesized patterned zeolite into active H-ZSM-5 phase through ion-exchange and calcination. On the other hand, the used methods differ in the way the ZSM-5 precursor is applied to the substrate.

All methods consist of the following few steps. First, a substrate is prepared for patterning after which a zeolite precursor solution is applied onto the surface. Then, the attached zeolite precursor is converted into zeolite through a hydrothermal step. This is followed by cleaning and calcining the as-synthesized micropatterned zeolite films to remove organic template. Finally, ion exchange is performed followed by calcination to transform the Na-ZSM-5 into H-ZSM-5.

Synthesis gels has been prepared in glass vials (for acidic solutions) and polypropylene tubes (for alkaline solutions) through stirring with Teflon coated magnetic stirring bars. Stirring bars have been cleaned through immersion in a mixture of nitric acid and hydrochloric acid (1:3 molar ratio) overnight.

3.2 Substrate preparation

A number of different substrates have been used and tested in the different methods to fabricate a ZSM-5 model system.

3.2.1 Substrate choice

Table 1 displays an overview of the properties of the different substrates. Silicon based substrates are not inert during crystallization of zeolite precursor but actually take place in the reaction. Silicon groups from the surface can dissolve and form crystalline nuclei which form the basis for further crystal growth.

Table 1: Substrates used for micropatterned model synthesis

Substrate	**Properties**
Si, Siegertwafer	Thickness: 525 µm, <100> orientation
Si coated with Si_3N_4 , Siegertwafer	Thickness: 525 µm + 100 nm Si_3N_4, <100> orientation
Si coated with SiO_2, Siegertwafer	Thickness: 525 µm + 100 nm (wet) SiO_2, <100> orientation
Borosilicate glass	
CaF_2	

First, the silicon based substrates were cut into squared 5 mm by 5 mm wafers using a diamond scriber. Then the surface was cleaned in a number of steps: nitrogen flow was used to blow off solid particles followed by washing in a solution of ethanol (96%, Sigma-Aldrich), acetone (97%, Sigma-Aldrich), and demineralized water (EtOH:Ace:H_2O = 1:1:1 volume ratio) in an ultrasonic bath for 15 minutes to remove of organic impurities of the surface. Next, the wafers were cleaned in demineralized water in an ultrasonic bath for 15 minutes to remove the solvents used in the previous cleaning step.

Afterwards, the surface was hydroxylated by heating to ≈333 K for 30 minutes in a mixture of hydrogen peroxide (30w% in water), ammonia (37w% in water) and demineralized water (H_2O_2: NH_3:H_2O = 1:1:5 volume ratio). This was followed by washing with demineralized water at ≈373 K for 30 minutes.[59] This step a fully, homogenously hydroxylated surface which is ready for subsequent modification steps to enable micropatterning of the surface.

After these hydroxylation steps, the wafers were dried in an oven (393 K) and transferred to a glovebox. Here, the wafers were immersed in a toluene solution (molecular sieve grade, 99%, Sigma-Aldrich) containing 0.01 M of octadecyltrichlorosilane (ODTS, 97.0%, Sigma-Aldrich), under N_2 atmosphere to prevent hydrolysis of ODTS with water present in air. As a result, self-assembled ODTS monolayers were formed on the substrate which transformed its surface from being of hydrophilic nature to hydrophobic due to the long hydrophobic, aliphatic chains.

3.2.2 UV ozone treatment

This newly formed hydrophobic monolayer of ODTS is necessary to enable successful patterning of the surface with zeolite. Bonding of hydrophilic zeolite precursor solution is not possible when the surface is blocked by hydrophobic chains and thus these have been removed using UV ozone treatment for 30 minutes. By protecting the surface with a copper grids such as TEM grids, certain areas of hydrophobicity can be protected against UV ozone treatment leading to a pattern of alternating hydrophobic and hydrophilic areas. Initially, a copper grid with squared holes (40 μm*40 μm) and approximately 20 μm distance between holes was used to pattern the wafers. In order to increase the distance between patterns as well as enable micropatterning of circular islands, a grid with circular holes (ø=20μm) was used. After UV ozone treatment, the substrate preparation was complete and the different zeolite precursor application methods were started.

3.3 Silica spin-coating

The first method to fabricate a model system of micropatterned zeolite thin films which has been explored is the synthesis of SBA-15 through spin-coating of a colloidal solution onto the prepared silicon-based substrates followed by hydrothermal crystallization into zeolite material. Further recrystallization of mesoporous SBA-15 would lead to microporous ZSM-5.

Firstly, a polymer solution was prepared by dissolving a mesoporous organic template, P123 (M_n=5800, Sigma- Aldrich) in ethanol (99.5%, Fisher BioReagents) while stirring for 2 hours at room temperature. Afterwards, demineralized water, an acidic catalyst, hydrogen chloride (HCl, 37%, Sigma-Aldrich) and a silica source, tetraethyl orthosilicate (TEOS, 99%, Sigma- Aldrich), were added.

The molar ratio of the reactants is: [47]

TEOS:H_2O:EtOH:HCl:P123 = 1 : 15.1 : 38.1 : 0.16 : 0.01.

The composition of the colloidal solution has been varied and its impact on the degree of spin-coating has been examined. After addition of TEOS (t=0), condensation started and the silica network had begun to form. At different moments after injecting TEOS (t=5 min. till t=4h), prepared wafers were spin-coated with the colloidal solution (3000rpm for 30 s). The wafers were first cleaned by spin-coating 20 µl of ethanol followed by the patterning through spin-coating 10 µl of colloidal solution.

A number of parameters have been varied such as the composition of the colloidal solution, in particular the amount of catalyst HCl, the spin-coating parameters, in particular the rotation speed and the amount of mixing time after adding TEOS, which is referred to as gelation time. Appendix A (section 9.1) provides an overview of the different tests.

After spin-coating the micropatterned wafers were calcined in an air oven for 5 h at 823 K with a temperature ramp of ≈2.0 K/ min to remove the organic template P123, which results in mesoporosity. However, the incorporation of aluminium into the SBA-15 structure is difficult to achieve. Therefore, SBA-15 usually lacks the intrinsic acidity of zeolites and thus its catalytic activity. [60]

3.4 Direct-dipping hydrothermal synthesis

The second method used to apply zeolite precursor onto the micropatterned substrate is the direct dipping in synthesis gel followed by a hydrothermal step. First, a basic synthesis gel was formed by mixing a template, tetrapropylammoniumhydroxide (TPAOH, 40w% in H_2O, Alfa Aesar) with demineralized water and adding sodium aluminate $NaAlO_2$ (40-45 w% Na_2O & 50-56 w% Al_2O_3). After mixing the solution for 30 min., TEOS was added and the final clear gel was stirred for 2 hours before being charged into a Teflon-lined autoclave (23 ml, figure 16). The final solution has the molar ratio: [26]

TEOS/TPAOH/$NaAlO_2$/H_2O = 0.8 : 0.1 : (0-0.08) : 50

which translates to a silica to alumina ratio of Si/Al=10 till Si/Al=∞. Micropatterned model systems have been prepared with a theoretical Si/Al ratio of Si/Al: 10,20,30,40,60,80,160,200 & ∞. A prepared wafer was placed at the bottom of the autoclave and hydrothermal reaction was carried out at 393 K for 12 h, 15 h or 24 h.

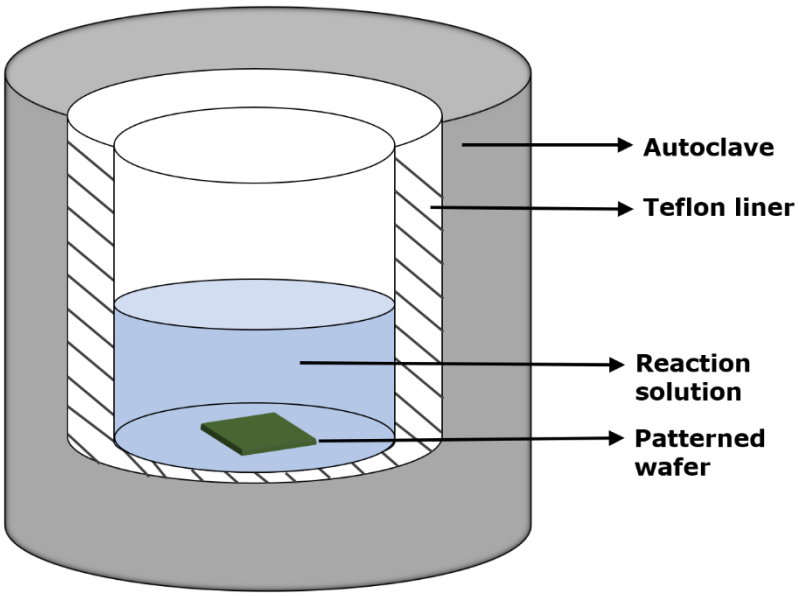

Figure 16: Schematic diagram of the direct-dipping hydrothermal synthesis method.

After the hydrothermal step, the wafer was rinsed in the ultrasonic bath for 5 minutes to get rid of loose zeolite crystals which were not covalently bound to the surface. Then the wafers were calcined in an air oven for 5 h at 823 K with a temperature ramp of ≈ 2.0 K/min to remove the template, TPA^+. Afterwards, ion exchange has taken place by immersing the wafer in an ammonium nitrate solution (1.0M NH_4NO_3, 98%, Sigma- Aldrich) for 2h up to 18h while stirring at 343 K. After one cycle, the wafers were rinsed intensively with water and the ion exchange was repeated up to four cycles.

In this step, as-synthesized zeolite containing sodium as cation, e.g. Na-ZSM-5, was converted to the ammonium state NH_4-ZSM-5 which was subsequently converted to H-ZSM-5 through calcination (5 h at 823 K). The micropatterned wafers have been characterized using optical microscopy, SEM, XRD & AFM.

After synthesis, the Teflon liners were rinsed with water and cleaned by scrubbing using the abrasive CIF. Then the Teflon liners were stored in a potassium hydroxide solution (2M) which helped dissolve any residual zeolite traces.

3.5 Spincoating ZSM-5 precursor under basic conditions

Another method which has been explored is the spin-coating of ZSM-5 precursor solution and crystallizing it directly into ZSM-5 through a hydrothermal step. Advantages of this method compared to spin-coating SBA-15 precursor is that it requires one step less since most components necessary are already spin-coated into one island and thus only one hydrothermal step is required.

First, a precursor solution was prepared by dissolving TEOS in ethanol and mixing TPAOH with H_2O and an aluminium source, such as $NaAlO_2$. After 1h of stirring, the silica and alumina precursor solutions were added together. The final solution has the following molar ratio: [61]

TEOS/TPAOH/$NaAlO_2$/H_2O/EtOH = 0.8 : 0.29 : (0-0.08) : 15 : 3.2

This final solution has a higher concentration of silica, alumina and template which is necessary to enable crystal growth localised on the islands after spin-coating. To facilitate spin-coating of the solution and investigate the influence of alcohol on the thickness of the islands, the final solution has also been diluted at least twice with methanol, ethanol or 2-propanol and the effect of the alcohol has been investigated. After two hours of stirring the final solution, the prepared substrates (SiO_2 coated Si wafers) were spin-coated at 2800 rpm for 30s with an acceleration of 100 rpm/s. First, the substrate was cleaned by spin-coating 20 µl ethanol (3000 rpm, 30 s) followed by spin-coating 10 µl of the precursor solution.

Spin-coated wafers have been transferred into a Teflon-lined autoclave on a Teflon pedestal (figure 17) and a small amount of water has been added to initialize the crystallization process in the hydrothermal step (20 µl to 200 ul). Hydrothermal reaction of the spin-coated samples was carried out at 423 K for 3 days. This was followed by calcination at 823K for 4h with a temperature ramp of 1.0 K/min. At last, the wafers were ion exchanged and calcined to obtain H-ZSM-5 according to the same procedure as in section 3.3.

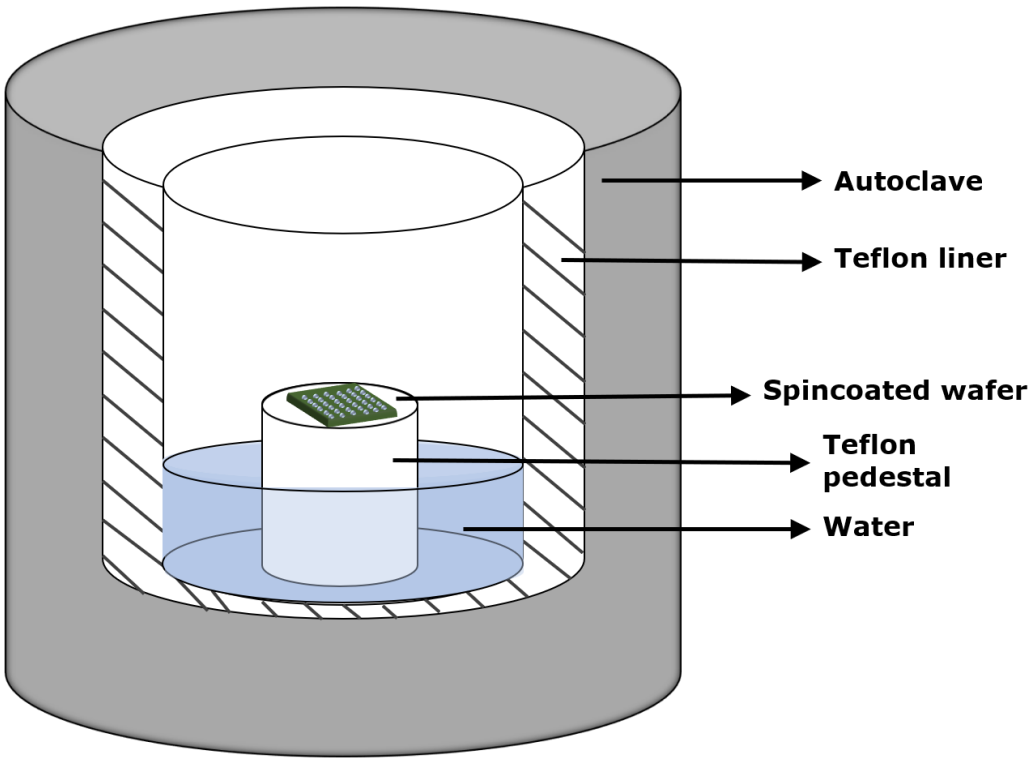

Figure 17: Schematic diagram of the hydrothermal step after spin-coating of ZSM-5 precursor solution.

3.6 Spincoating ZSM-5 precursor under neutral conditions

Contrary to the synthesis gel used in the direct-dipping method, it has shown to be important for the aluminium source to dissolve in the mixture used for spin-coating of ZSM-5 precursor solution. In a micropatterned model system, each island of zeolite needs to possess the same Si/Al ratio. In order to optimize dissolving of an aluminium source and to ensure a homogenous concentration of aluminium throughout the model system, ZSM-5 precursor has been spin-coated under neutral conditions. Similar to spin-coating under basic conditions, TEOS was first dissolved in ethanol while simultaneously a solution of water, tetrapropyl ammoniumbromide (TPABr, 98%, Sigma-Aldrich), and aluminium chloride hexahydrate ($AlCl_3.6\ H_2O$, 99%, Fluka Analytical) was prepared. After addition of the silica and alumina precursor solutions, the mixture was stirred for 2 hours before spin-coating onto the prepared substrates (SiO_2 coated Si wafers). The spin-coating procedure is similar to the procedure under basic conditions (chapter 3.4).

Thereafter, the spin-coated wafers were transferred onto a pedestal in a Teflon-lined autoclave and hydrothermal reaction has taken place involving the addition of a base which provides a mobilizing agent (OH^-). Different amounts of ammonia solution (28%, Sigma-Aldrich) and H_2O have been added (from 20 µl to 500 µl). After the hydrothermal reaction in an air oven (423 K for 3 days), the wafers were calcined at 823K for 4h with a temperature ramp of 1.0 K/min. At last, the wafers were ion exchanged and calcined to obtain H-ZSM-5 according to the same procedure as in section 3.3.

3.7 Microinjecting ZSM-5 precursor

A final method which has been explored to fabricate a micropatterned zeolite thin film model system is the micro-injection of basic and neutral ZSM-5 precursor solution onto a substrate. In this method, a basic precursor solution and a neutral precursor solution have been prepared in a similar manner as in chapter 3.4 & chapter 3.5. These precursor solution contained varying Si/Al ratios of Si/Al=20,40,80,160 & ∞.

These solutions have been manually deposited onto a substrate using a microneedle (Eppendorf FemtoJet 4x) while observing the patterning through an optical microscope (ZEISS Axio Observer). Microneedles have been prepared. Before microinjection, the solutions were filtered using a 0.45 µm membrane filter (Thermofisher) to remove any agglomerates, impurities or undissolved (aluminium) species. To ensure a homogenous distribution of aluminium species in every island, a neutral precursor solution has been prepared in which the aluminium species fully dissolved.

Because this method applies manual microinjection, more freedom in the choice of substrate was possible and thus different substrates have been used than were used for spin-coating and direct hydrothermal synthesis. The ZSM-5 precursor solutions have been microinjected onto wafers of borosilicate glass and calciumfluoride. Borosilicate glass has been prepared by either cleaning with ultrasonication, cleaning followed by hydroxylation or cleaning followed by hydroxylation and patterning as described in chapter 3.2. Calciumfluoride substrates have been prepared by cleaning with ultrasonication.

3.8 Characterization methods

3.8.1 Optical Microscopy

During the different steps in the fabrication of the micropatterned ZSM-5 model system, optical microscopy has been used to quickly identify the degree of micropatterning, spin-coating and crystal growth of the micropatterned zeolite thin film. An Olympus microscope has been used with magnifying lenses of 5*, 10* and 50* magnification. Throughout the process of optimizing the model system, different microscope lenses and settings (light) have been used meaning that model systems are not compared with each other in terms of e.g. their colour.

3.8.2 X-Ray Diffraction

X-ray diffraction (XRD) has been used to confirm the presence of zeolite phase in the synthesized micro-patterned ZSM-5 thin films. Diffraction patterns have been collected using a Bruker D2 Phaser (2nd Gen) instrument using a cobalt radiation source, Co k_{alpha} = 1.789 Angstrom.

The standard XRD program to detect whether a sample contained MFI zeolite (ZSM-5) had an angle range of 5-50° with an increment of 0.05 and measuring time per step was 1 second.

3.8.3 Scanning Electron Microscopy

Scanning electron microscopy (SEM) has been used obtain information of the topography and morphology of the synthesized zeolite patterns. The Phenom ProX scanning electron microscope has been used for imaging and analysis using both 10kV and 15kV acceleration voltages. Samples have been prepared by sticking the wafer onto an aluminium pin using carbon adhesive discs (Agar scientific).

3.8.4 Atomic Force Microscopy

Atomic force microscopy (AFM) has been used to obtain information on the crystalline properties of the synthesized model. AFM images have been scanned with PeakForce Tapping Mode and Contact Mode at scanning frequencies of 2 kHz and 4 kHz. Different probes have been used as tips including High Accuracy NonContact probes (HA_NC, NT-MDT Spectrum Instruments), Single Crystal Diamond probes (SCD14/AIBS, MikroMasch) DP15/GP/No Al and HQ:NSC_14/No Al.

3.9 Catalysis

3.9.1 Confocal Fluorescence Microscopy FM: 4- fluorostyrene oligomerization

The oligomerization of 4-fluorostyrene catalysed by synthesized micropatterned ZSM-5 has been investigated through fluorescence measurements conducted using a Nikon ECLIPS 90i upright confocal laser scanning fluorescence microscope.

3.9.2 Methanol-to-olefin

The methanol-to-olefin reaction catalysed by the synthesized micropatterned ZSM-5 has been investigated using in-situ UV/VIS absorption spectroscopy as well as on-line Mass Spectrometry (MS). A flow of 10.00 ml/min N_2 is applied to a sealed reactor cell containing the micropatterned wafer. After heating to 393K (30 K/min ramp) for 1h followed by heating to 623K (30 K/min ramp) at 2h, all present oxygen has been removed and the reaction was started by flowing the nitrogen through methanol. The presence of coke species as well as olefins has been monitored using UV/VIS and MS.

Chapter 4 – Results and discussion

In this study of designing a micropatterned model system, initial findings have provided an increasing understanding of the requirements of the model system and the improvements which can be implemented. Synthesized micropatterned zeolite (precursors) have been characterized through optical microscopy, SEM, AFM & XRD measurements. The results are reported per method used.

4.1 Spin-coating of SBA-15 precursor under acidic conditions

Spin-coating of SBA-15 precursor solution has been performed after certain time intervals after addition of TEOS to the colloidal solution. Microscopic images have been taken of wafers spin- coated with the colloidal solution after different gelation times ranging from 5 minutes to 4 hours. Some factors that influence the quality of the spin-coated micropatterned films are the composition of the solution, gelation times and spin-coating settings. The sol-gel composition has been based on the synthesis of mesoporous silica thin films by Kato et al.[47] Appendix A shows an overview of the different parameters that have been tested and have led to a micropatterned film.

4.1.1 Influence EtOH/H_2O ratio

Firstly, the composition of the colloidal solution has been altered by changing the water to ethanol ratio. This ratio has been tested in the range of

EtOH/H_2O= 0.3 till EtOH/H_2O= ∞

Which means addition of an excess of water till no addition of water but only ethanol. Altering this ratio influences the viscosity of the colloidal solution as well as its behaviour during spin-coating; ethanol evaporates more rapidly than water. Many different ratios have resulted in successful patterning of the colloidal solution onto a substrate and thus no connection has been found between these parameters. As explained in section 2.2.1, water molecules are required to initiate hydrolysis and ethanol mainly acts as solvent for water and TEOS, which are immiscible. Once hydrolysis is followed by condensation, a water molecule has become available to re-initiate the cycle again.

According to this reasoning, no water should be available for hydrolysis when EtOH/H_2O=∞ and gelation should not occur. However, this is opposed to the visual observation that the viscosity of the colloidal solution has increased over the course of a few hours. Moreover, figure 18 shows successful partial patterning of the colloidal solution after 3h of gelation, without addition of H_2O. Spin-coating of a control colloidal solution without TEOS has not resulted in successful patterning which suggests that a silica network had been formed before spin-coating the sample in figure 18.

Possible reasons for this observations could be the presence of water molecules in the catalyst (HCl, 37w% in H_2O). This equals an actual ethanol to water ratio of $EtOH/H_2O \approx 50$ which could provide enough H_2O to initialize hydrolysis and gelling of the colloidal solution. Additional sources of H_2O include moisture from air and impurities of involved solutions but this is expected to play a smaller role than addition of catalyst.

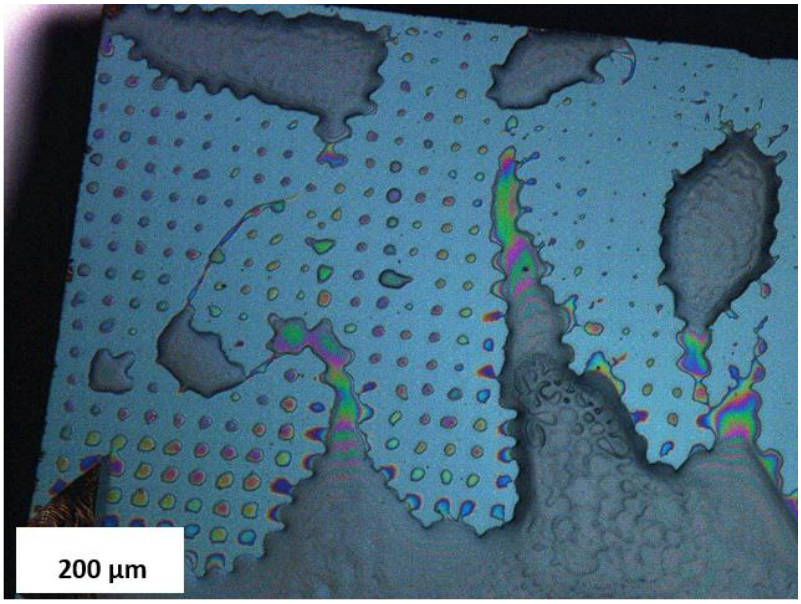

Figure 18: Optical micrograph of spin-coated colloidal solution with $EtOH/H_2O=\infty$ on a Si substrate after 3h gelation time. Six times as much catalyst as in lit. has been used.

4.1.2 Influence catalyst & gelation time

Secondly, the composition of the colloidal solution has been altered by changing the amount of catalytic hydrochloric acid added to the colloidal solution. This amount has been compared to literature[47] and this ratio has been tested in the range of $HCl_{added}/HCl_{literature}$ = [0.4 : 32] which equals a ratio of TEOS:HCl = [2.5 : 200].

Besides $HCl_{added}/HCl_{literature}$ = 0.4, use of almost all other different catalyst ratios has resulted in successful (partial) patterning of substrates (chapter 9.1). This indicates that formation of a silica network through hydrolysis and consecutive condensation occurs as long as enough catalyst has been added. However, adding low amounts of catalyst have resulted in a low rate of gelling of the colloidal solution which means that even though for HCl_{add}/HCl_{lit} =0.4, the gelation might have started, it was still not observable after 4h of gelation. Since the rate of the reaction increases upon addition of more catalyst, the gelation time decreases before the same size or degree of 3D silica network has been formed.

This is supported by figure 19 showing partial micropatterning after 5h at low catalyst amount and figure 20 showing partial micropatterning after 16 min but not after 3h. Instead, the latter shows a thick film spin-coated onto the substrate with relief indicating the presence of a viscous 3D silica network. One could note that at low acid concentrations, a thin film is also formed at low gelation times. The difference between these films is that after 16min, it mainly consists of solvent such as ethanol which has not been evaporated yet, possible due to the spin-coating settings. While at 300min, the film does not appear

to be homogenous and flat but rather bulky. Please note that the difference in colours is due to the use of different microscopes.

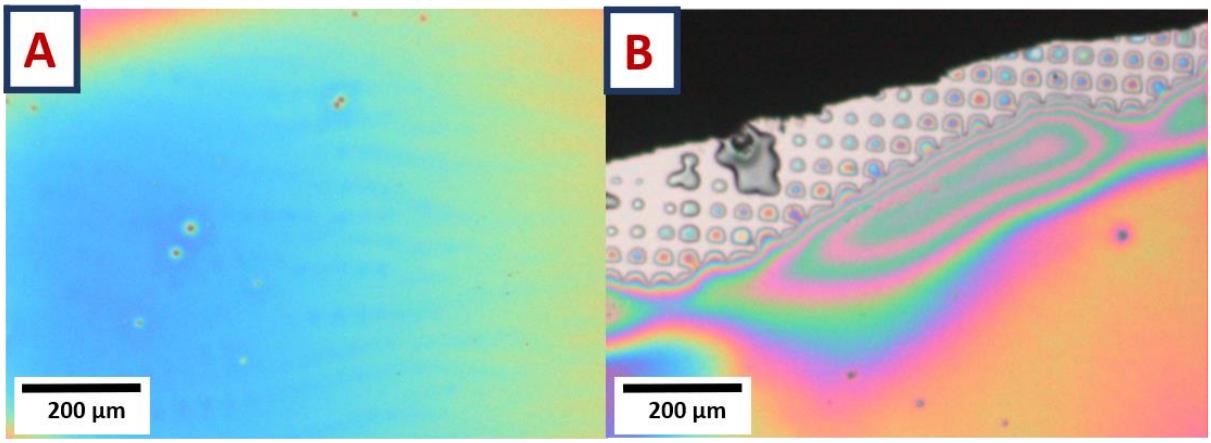

Figure 19: Optical micrograph of spin-coated colloidal solution. a) after 16 min, b) after 300 min. EtOH/H_2O = 5.4. Six times as much catalyst as in ref. [47] has been used.

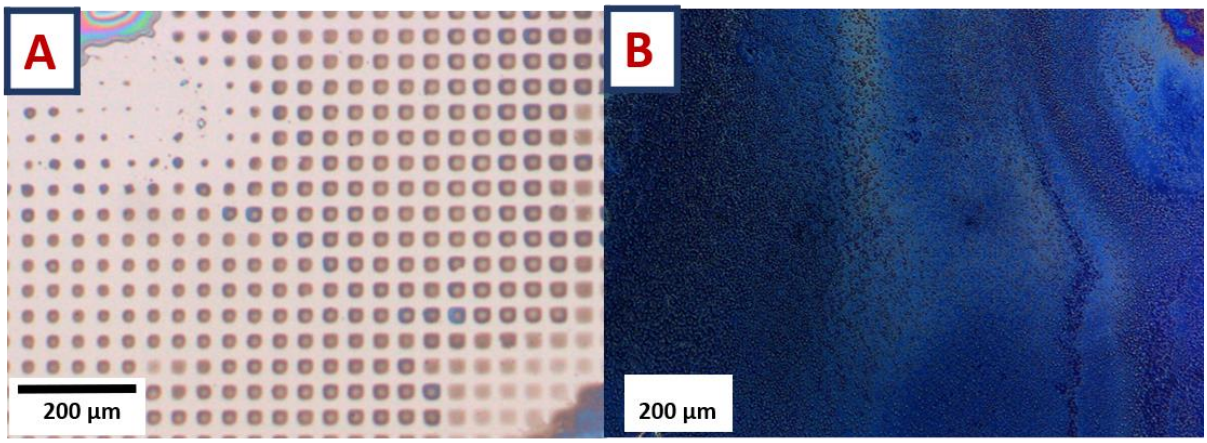

Figure 20: Optical micrograph of spin-coated colloidal solution. a) after 15 min, b) after 180 min. EtOH/H_2O = 5.4. 32 times as much catalyst as in ref. [47] has been used.

4.1.3 Influence spin-coating settings

The quality of the micropatterned substrate is not only dependent on the composition of the colloidal solution but also on the settings of the spin-coating procedure. Three parameters have been investigated including the rotating speed of the disc, the duration of spin-coating and whether the substrate was stationary or rotating while depositing the solution. One programme which has been used consist of addition of the colloidal solution before rotation, then a step of 5 s rotating at 500 rpm to ensure proper spreading on the substrate followed by 30 s rotation at 3000 rpm to evaporate the solvent.

When depositing the colloidal solution while rotation had started, incomplete spreading of the substrate occurred possibly due to incorrectly deposition the solution next to the middle instead of in the centre or because incorrect deposition removes the solution in the centre of the substrate due to a puff of air.

Overall, spin-coating of colloidal solution has led to irreproducible results depending on small differences in composition or gelation time as well as physical conditions such as wafer cleaning steps.

4.2 Direct-dipping Hydrothermal synthesis

In the second method which has been explored, micropatterned ZSM-5 thin films have been fabricated through direct-dipping hydrothermal synthesis. Some factors that influence the micropatterned model systems include the composition of the synthesis gel, reaction conditions and the influence of the substrate.

The influence of the composition of the synthesis gel has been explored by altering the concentration of template, TPAOH, and the silica to alumina ratio by adding more Al containing precursor while obtaining a constant silica to water ratio. The synthesis gel is based on a study by Ha et al [26] and the molar ratio between its components is equal to TEOS/TPAOH/$NaAlO_2$/H2O = 0.8 : 0.1 : (0-0.08) : 50.

4.2.1 Influence of template

Firstly, the influence of the template has been investigated by altering the amount of template added to the synthesis gel. This amount has been compared to literature and this ratio has been tested in the range of $TPAOH_{added}/TPAOH_{literature}$ = [0.4 ; 1.5]. Each synthesis gel contained a silica to alumina ratio of Si/Al = 160 and hydrothermal synthesis has been performed at 393 K for 12 h.

Figure 21 shows the optical image of micropatterned films after hydrothermal synthesis using synthesis gels with different concentration of template. When adding too much template (figure 21 A), the Si_3N_4 wafer partially degrades and an irregular micropattern is visible. Figure 13B shows a successfully patterned wafer but when the amount of template is even further decreased, patterning of the wafer is becoming incomplete and zeolite material is not bond to the substrate.

These observations are in accordance with the theory which states that TPA^+ acts as a structure directing agent and is involved in the synthesis of MFI zeolites. TPA^+ cations have been reported to form complexes with both silicate or aluminosilicate species as well as compensate with Na^+ cations for charge compensation which is required to counteract the negative charge caused when an alumina tetrahedron substitutes a silica tetrahedron in the zeolite framework.[62] When the requirement of sufficient template is not met, the crystallization rate slows down and this results in a lower quality of a micropatterned model system. An effect which accompanies a reduction of template is a reduction in amount of OH^- anions added and thus an increase in pH. Alkalinity plays an important role in zeolite synthesis; reducing the pH leads to lower crystallization rates an increased induction times. However, it is also reported that at high pH values, silica is more likely to dissolve and remain in liquid phase instead of becoming incorporated into a crystalline solid phase.[63] This means that additional experiments must be performed to investigate the influence of the pH and that it may be suggested that the observations are caused by the reduction of the template concentration.

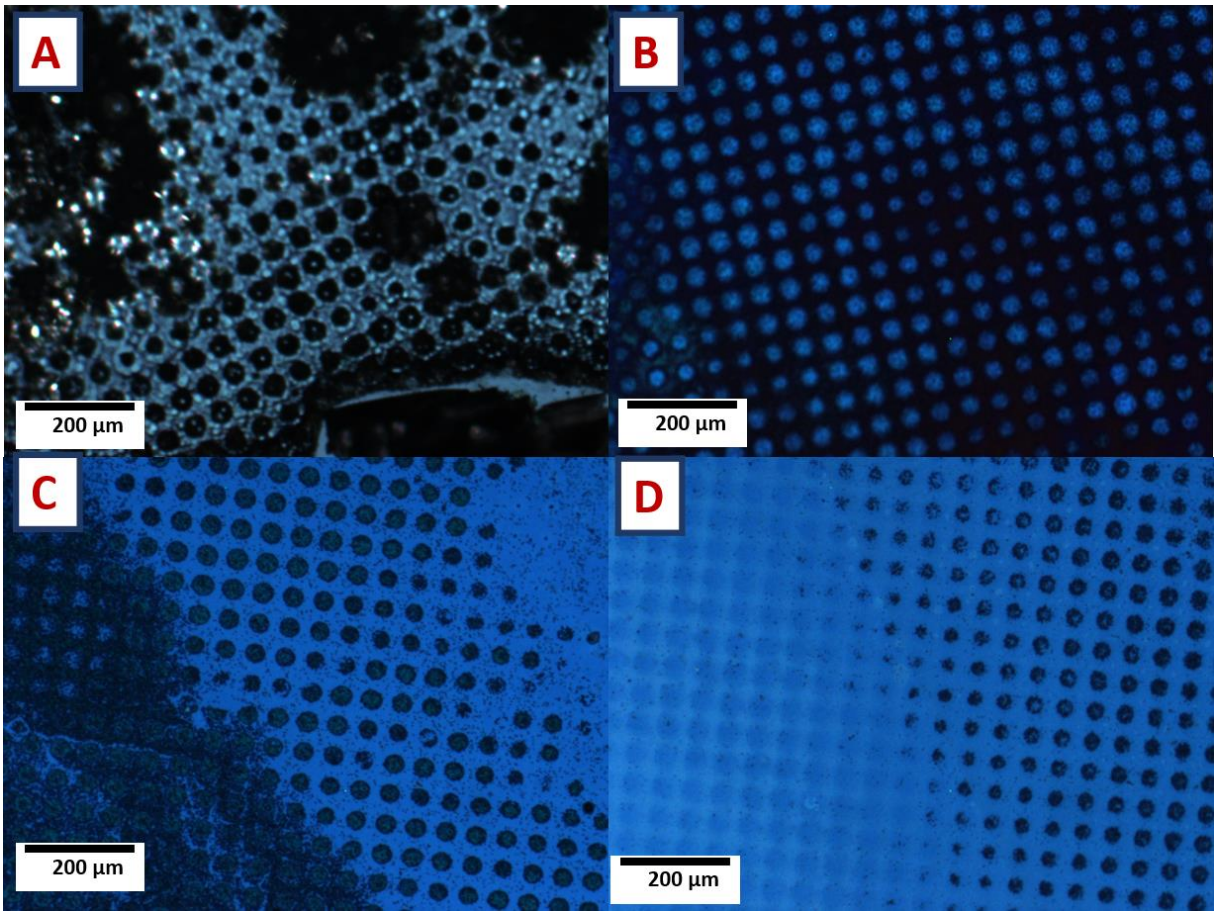

Figure 21: Optical micrograph of micropatterned films (Si/Al= 160) on a Si_3N_4 coated Si wafer through direct-dipping hydrothermal synthesis. $TPAOH_{added}/TPAOH_{lit}$ =A) 1.5, B) 0.75, C) 0.6, D) 0.4. Hydrothermal step of 12 h at 393 K

4.2.2 Influence Si/Al ratio

Secondly, the influence of the template has been investigated by altering the silica/alumina ratio of the synthesis gel. The synthesis of ZSM-5 is a versatile process and researchers have successfully synthesized it with Si/Al ratio in the range from Si/Al= 10 – 1000. In this study, micropatterned zeolite films have been synthesized with a Si/Al ratio in the range of Si/Al= 10 - 200 and Si/Al= ∞ which corresponds to the synthesis of purely siliceous SM-5, silicalite-1. Figure 22 shows the optical image of micropatterned films after hydrothermal synthesis using synthesis gels with different Si/Al ratios (200,120,60 & 30) At high Si/Al ratios, the crystalline material has attached to the substrate on distinct areas creating a high quality of micropatterned zeolite film (figure 22 A & B). When decreasing the Si/Al ratio by incorporating more alumina, the quality of patterning decreases and a thin film is grown rather than a micropatterned film (figure 22 C & D). This overgrowth can be assigned to an increase in nucleation which is caused by Al^{3+} cations, which favour nucleation over crystal growth, contrary to a purely siliceous system.[64] Since TPA^+ primarily forms organic-inorganic bonds with silicate species, aluminate is not properly incorporated into the framework but is rather left outside the formed crystal, called Al-zoning. This results in random nucleation outside of the patterned regions. This problem can be solved by replacing TPA^+ by another structure directing agent.[17]

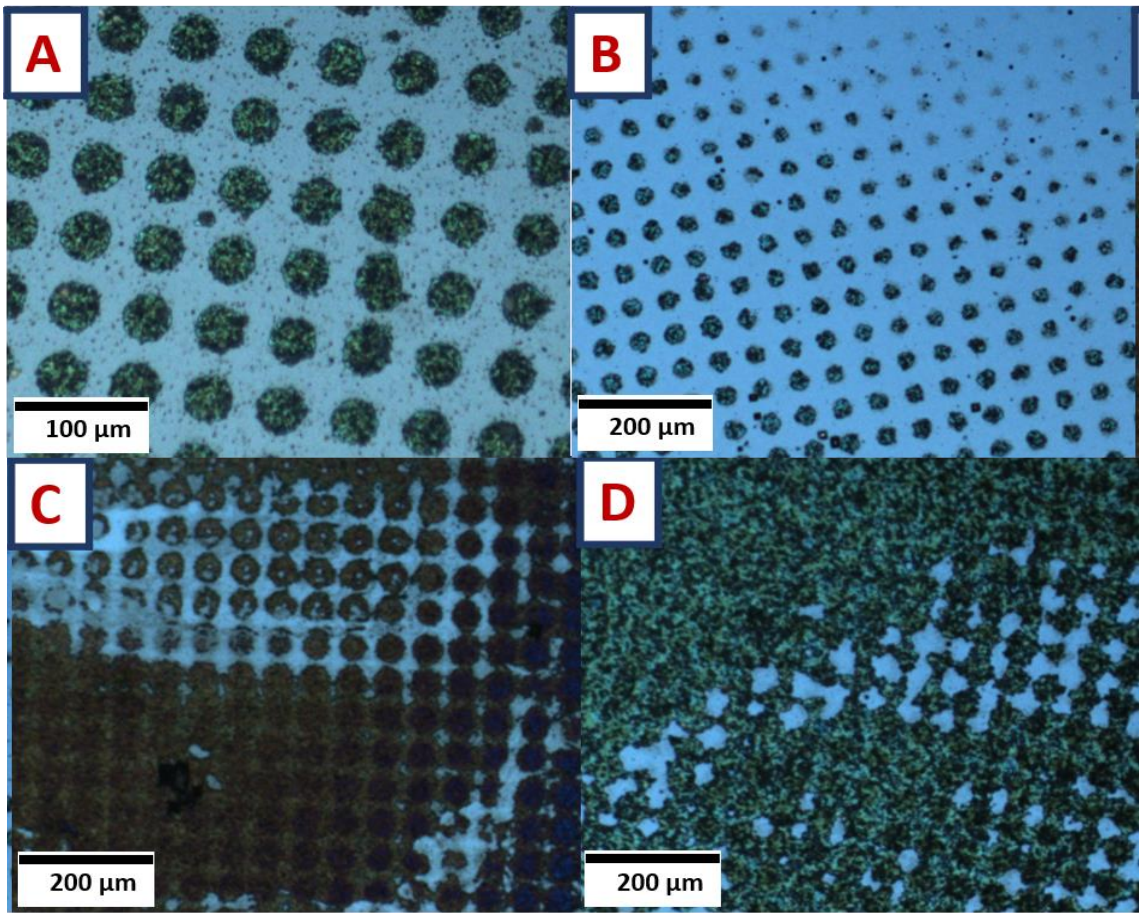

Figure 22: Optical micrograph of micropatterned films on a Si_3N_4 coated Si wafer through direct-dipping hydrothermal synthesis. Si/Al= A) 200, B) 120, C) 60, D) 30. Hydrothermal step of 12 h at 393 K

Figure 23 shows the optical image of micropatterned films after hydrothermal synthesis using synthesis gels with low Si/Al ratios and thus high amounts of aluminium present. When the Si/Al becomes too low (B: Si/Al=10), the presence of aluminate species becomes too dominant and prevents facile growth of MFI crystals attached to the Si based substrate. When too much aluminium is present in the synthesis gel, formation of zeolite crystals may not occur at all.

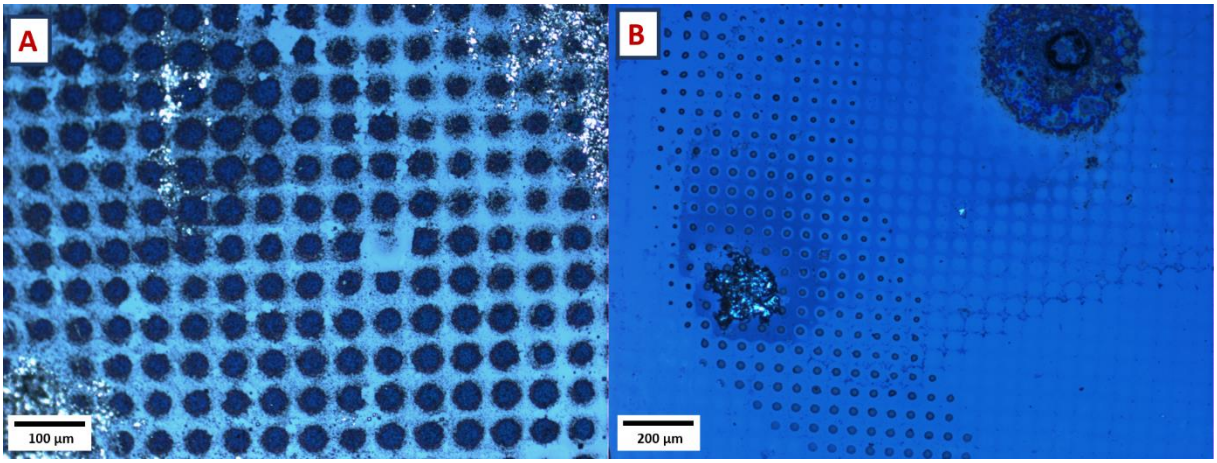

Figure 23: Optical micrograph of micropatterned films on a Si_3N_4 coated Si wafer through direct-dipping hydrothermal synthesis. Si/Al= A) 20, B) 10. Hydrothermal step of 12 h at 393 K

The influence of the Si/Al ratio in the crystal formation and shape of the micropatterned zeolite model system has also been explored using SEM & AFM. Figure 24 shows the optical micrograph, SEM & AFM of a micropatterned film with Si/Al=∞. The circular areas of crystalline material are well separated and hardly any crystals have bonded to the background of the wafer. SEM micrograph shows coffin shaped crystals which are in accordance with known MFI crystal shape. [65] SEM and AFM show presence of a monolayer with multi-layered areas and crystals protruding from the bottom layer. When this crystalline island is compared to figure 25, a few observations are notable. First of all, after the introduction of aluminium (figure 25, Si/Al=160), more individual crystals have grown onto the wafer outside of the patterned area. This can be explained by referring to the ability of aluminium to increase nucleation. Moreover, SEM and AFM show multiple layers of crystalline material indicating an increased crystal growth and resulting in a higher total height of the island, which is supported by literature. Coffin shaped crystals are distinguishable but have grown together forming clusters of crystals pointing in multiple directions. Figure 26 shows a micropatterned zeolite thin film with Si/Al=40 which consists of multilayers of crystalline material as well.

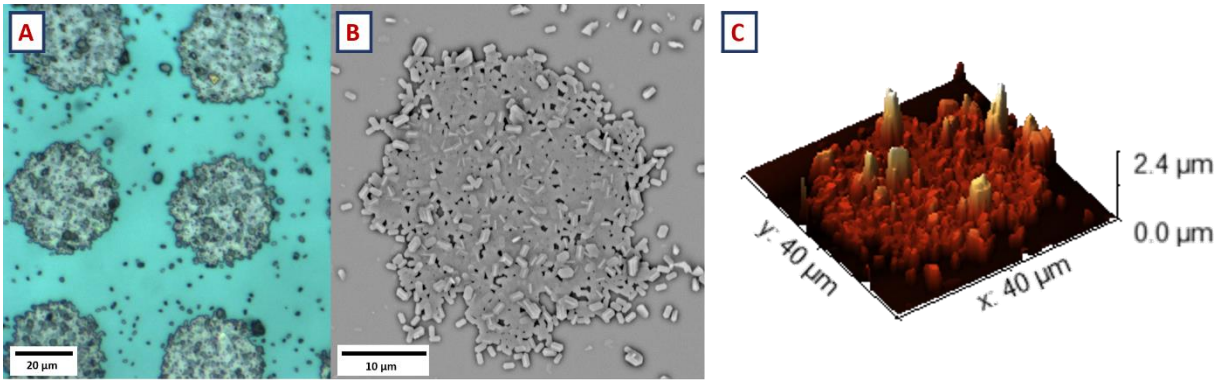

Figure 24: Optical micrograph, SEM & AFM of a micropatterned film (Si/Al= ∞) on a SiO_2 coated Si wafer through direct-dipping hydrothermal synthesis. Hydrothermal step of 24h at 393K.

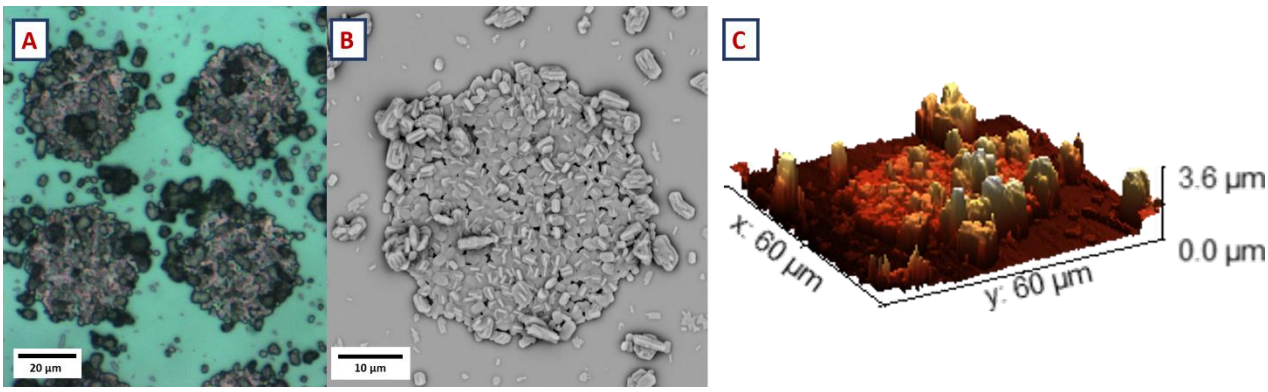

Figure 25: Optical micrograph, SEM & AFM of a micropatterned film (Si/Al= 160) on a SiO_2 coated Si wafer through direct-dipping hydrothermal synthesis. Hydrothermal step of 24h at 393K.

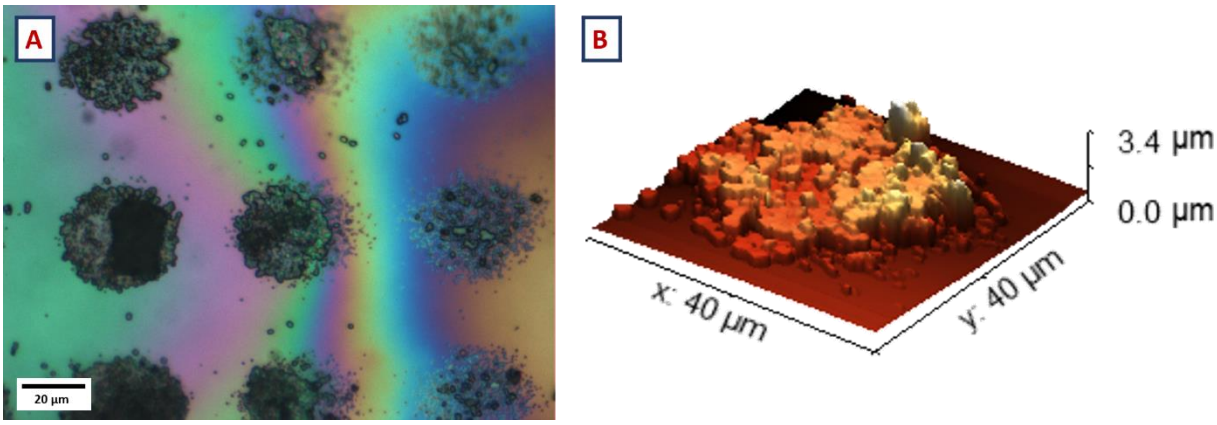

Figure 26: Optical micrograph & AFM of a micropatterned film (Si/Al= 40) on a SiO_2 coated Si wafer through direct-dipping hydrothermal synthesis. Hydrothermal step of 24h at 393K.

4.2.3 Influence reaction temperature

The influence of the reaction conditions on the synthesis of micropatterned zeolite thin films through direct-dipping hydrothermal synthesis has been investigating by exploring both the reaction temperature and duration. The reaction temperature plays an important role in the crystal shape and formation of the micropatterned zeolite model system. Therefore, it has been explored in this study using optical microscopy, SEM & AFM.

Figure 27 shows the optical image, SEM & AFM of a micropatterned film with Si/Al=∞, synthesized at 453K for 4h. The micropatterned films shows high quality of patterning and practically no crystallization outside the patterned regions. SEM & AFM show a monolayer of narrow, coffin shaped crystals with a few crystals forming multilayers. When compared to figure 24, a similar model system has been synthesized in 4h at 453 K as has been synthesized in 24h at 393 K. This result suggests that for silicalite-1 synthesis, the crystallization rate increases at higher temperatures.

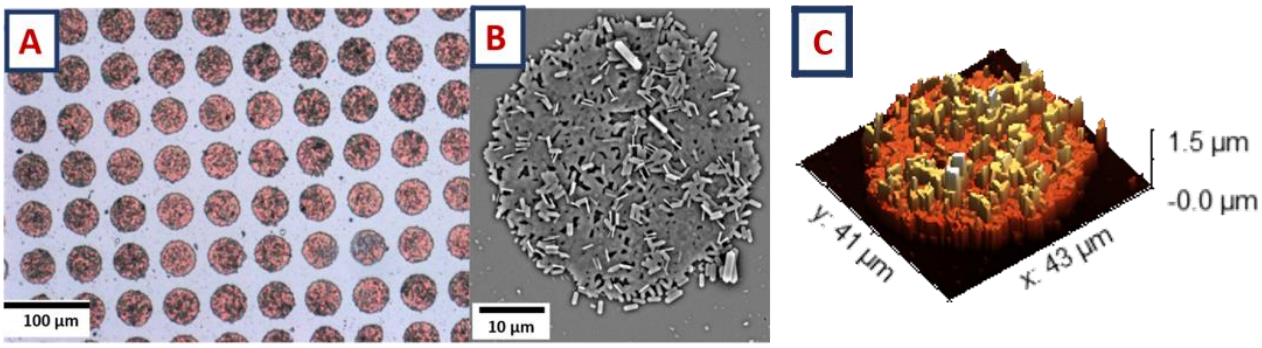

Figure 27: Optical micrograph, SEM & AFM of a micropatterned film (Si/Al=∞) on a SiO_2 coated Si wafer through direct-dipping hydrothermal synthesis.. Hydrothermal step of 4h at 453 K.

Cejka et al. states that increasing temperature increases both the rate of nucleation and crystal growth. However, these rates are not increased equally since the crystal growth rate will be increased in particular. This results in larger crystals and higher growth rates at high temperatures. Moreover, crystals consist of several facets, each with their own activation energy and thus their own reactivity. This means that upon elevating the temperature, some crystal faces are more prone to reaction than others and therefore the

aspect ratio changes. As a result of the changing aspect ratio, which is equal to the length of the crystal divided by its width, the crystal morphology can change.[9] This explains why figure 27 shows larger and narrower coffin shaped silicalite-1 (MFI) crystals than figure 24.

4.2.4 Influence reaction duration

Figure 28 shows the optical image and SEM of a micropatterned film with Si/Al=160, synthesized at 393K for 12 h. A monolayer of crystals is visible with a slightly coffin-like, squared shape. When compared to figure 25, both micropatterned zeolite films have been synthesized from identical synthesis gels at the same temperature but the reaction duration of figure 28 was twice as long as figure 25, 24 and 12 h respectively. The crystalline islands differ in a number of ways. For longer reaction durations, more zeolite material appears to have formed more multi-layered areas**.** Besides, the shape of individual crystals is different as well as the orientation. At shorter durations, a flat crystalline monolayer appears to have formed whereas at longer durations, crystals are oriented randomly and a lot of perturbing crystals are present. In general, crystallinity increases with time. However, zeolites are not always stable crystalline phases but exist as metastable phases which react consequently into more stable phases, according to Ostwald's law.[9] This could suggest that the differences in crystal shape are due to the a different zeolite state. Kinetics may not also not be forgotten which is supported by the differences between figure 25 & 28.

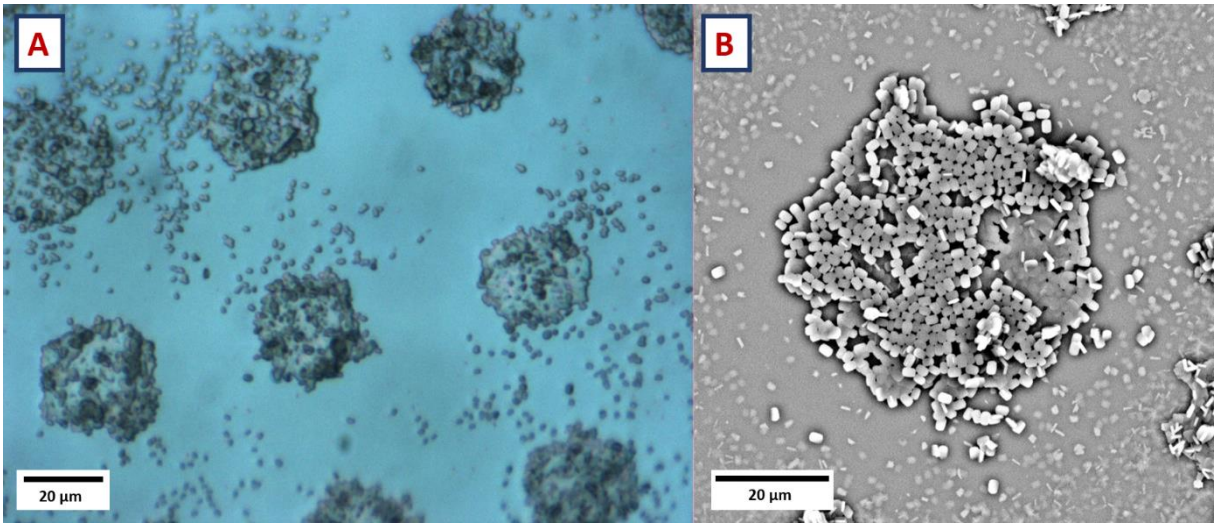

Figure 28: Optical micrograph & SEM of a micropatterned film (Si/Al= 160) on a SiO_2 coated Si wafer through direct-dipping hydrothermal synthesis.. Hydrothermal step of 12 h at 393 K

4.2.5 Influence of substrate

In zeolite synthesis, the substrate can play an important role in the crystallization process of the zeolite, especially when the zeolite is epitaxially grown onto a Si based substrate. In order to explore the influence of the substrate on the micropatterned zeolite thin film model through direct-dipping hydrothermal synthesis, a number of silicon based wafers have been micropatterned and analysed with optical microscopy, SEM, AFM and X-ray diffraction.

When micropatterning Si_3N_4 coated Si wafers through direct-dipping hydrothermal synthesis, the presence of black squares has been noticed (figure 29). These squares do not represent crystals grown onto the surface but rather the etching of the surface creating a valley-shaped dent. These defects occur both on the hydrophilic patterned areas as well as the hydrophobic regions between islands of zeolite and might be caused by the reaction of the surface groups present in the Si_3N_4 layer. This observation has led to the use of other substrates, such as uncoated Si <100> wafers and Si wafers coated with SiO_2.

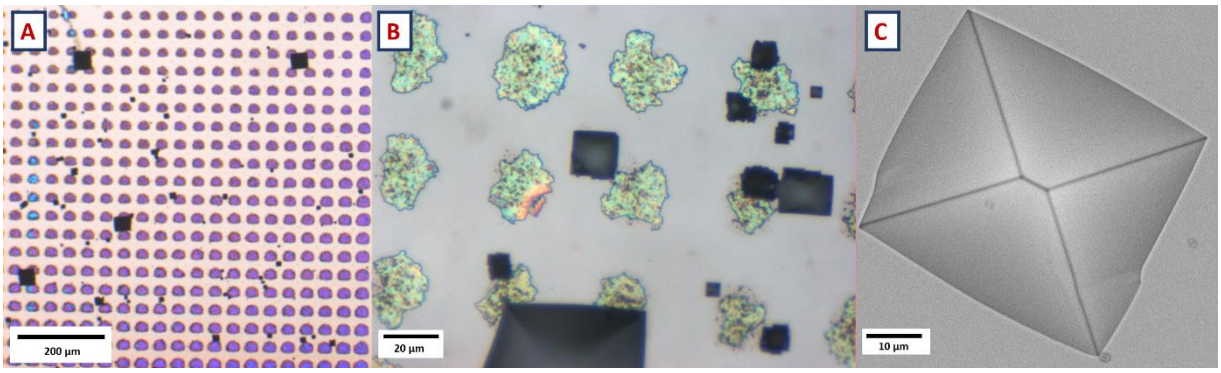

Figure 29: Optical micrograph and SEM of a micropatterned film (Si/Al=∞) on a Si_3N_4 coated Si wafer through direct-dipping hydrothermal synthesis. Hydrothermal step of 15 h at 393 K.

However, when uncoated Si wafers were submitted to direct-dipping hydrothermal synthesis, no micropatterned wafers were synthesized. Figure 30 shows the result of hydothermal synthesis on Si_3N_4 coated substrates (figure 30A, which shows squared defects) as well as hydrothermal synhesis under the same conditions on uncoated Si substrates (figure 30B). The entirety of the surface appears to have been degraded and affected during the reaction. Additional measurements have indicated that the prepared Si substrates appear to be intact after hydroxylation and that the degradation occurs during the hydrothermal step. Altering the synthesis gel (figure 30C, Si/Al=40) leads to similar observations of complete or partial degradation of the surface. A potential cause for this degradation could be that the uncoated silicon wafer is more reactive than the coated wafers since the framework silicon is more available under a thin layer of surface silanol groups whereas silicon nitride is known for its chemical inertness. [66]

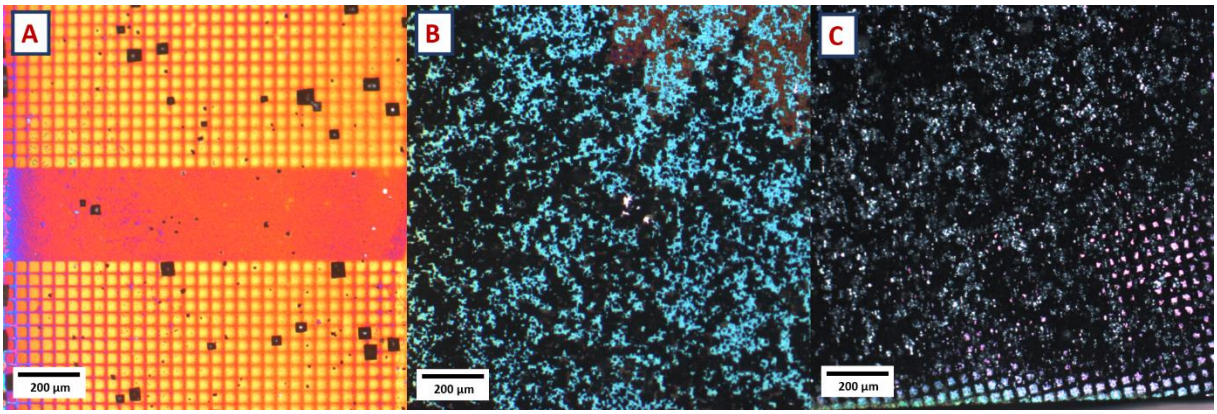

Figure 30: Optical micrograph of a micropatterned film (Si/Al=∞) on a Si_3N_4 coated Si wafer (A) and an uncoated Si wafer (B) in the same autoclave (12 h at 393 K) and micropatterned film ((Si/Al=40) on an uncoated Si wafer (C) (12 h at 393 K) .

SiO_2 coated Si wafers do not experience surface etching or degradation but result in micropatterned wafers (figure 24 till 27). Depending on the reaction conditions which have been discussed before, the micropatterned islands are defined and separate and crystal growth is limited to the hydrophilic areas containing surface silanol groups. Nonetheless, micropatterning of SiO_2 coated wafers has resulted in crystal growth exclusively inside the patterns, exclusively outside the patterns and in both areas. Figure 31 shows a wafer on which crystal growth appears to favour the hydrophilic areas while on other parts of the same wafer the hydrophobic areas appear to be favoured. A reason for this phenomenon could be that the incorporation of aluminium enables the formation of amorphous alumina and silica aggregates which are converted into zeolite crystals. [34] Moreover, contact with nuclei and the liquid phase is important to grow efficiently and thus nucleation does not only take place on the surface of the substrate but also in bulk solution. This could result in zeolite aggregates or crystals bonding with crystals attached to the surface, thus ignoring the hydrophobic surface groups and resulting in overgrowth or odd zeolite patterning.

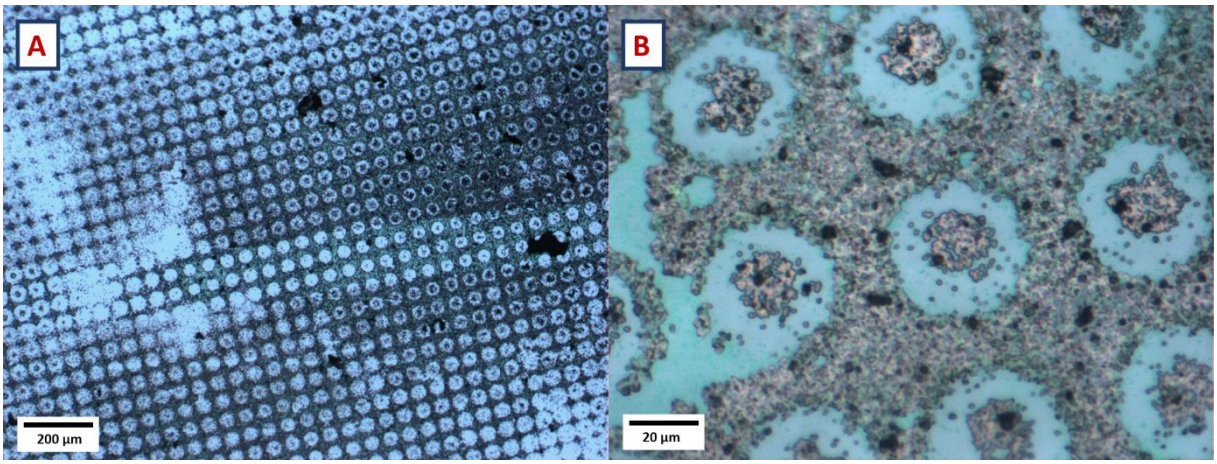

Figure 31: Optical micrograph of a micropatterned film (Si/Al= 40) on a SiO_2 coated Si wafer through direct-dipping hydrothermal synthesis. Hydrothermal step of 12 h at 393 K.

In order to prevent random crystal growth in the synthesis of a micropatterned zeolite thin film model system as well as achieve higher control over the distribution of crystal growth on the substrates, other methods such as spin-coating and microinjection have been explored. Moreover, a small research has been performed into the use of other chemicals to prepare a micropatterned substrate (section 9.2)

4.3 Spin-coating of ZSM-5 precursor solution

Spin-coating of ZSM-5 precursor solution has been performed followed by hydrothermal steaming resulting in the crystallization of patterned islands.

In this method, the condensation of the silica & alumina network in the solution takes place in a basic environment, contrary to spin-coating of a sol leading to SBA-15. As a result, the solution behaves differently and other spin-coating settings have been applied. To ensure better spreading during the spin-coating step, the precursor solution has been diluted with a number of alcohols. After hydrothermal steaming in an autoclave followed by calcination, the synthesized model system has been characterized using optical microscopy, AFM & SEM. There are number of factors which influence this process including the amount of water added in the hydrothermal step, the amount of alcohol used and the

4.3.1 Influence of water in hydrothermal step

Figure 31A shows the high quality of spin-coating of a basic precursor solution containing TEOS,H_2O, EtOH & TPAOH after 4h of stirring. In b & c crystallization at the edges of the patterns after a hydrothermal step of 3 days at 423 K is shown, whereas the centre of the island appears to contain unreacted precursor solution. SEM image confirms the synthesis of coffin shaped MFI crystals (figure 32) and the presence of fully crystallized islands as well as partially crystallized islands. A duplicate experiment using the same reaction conditions is shown in figure 33. Contrary to previous findings, crystallization seems to have completed fully and a monolayer of coffin shaped MFI crystals has formed. However, growth of crystals outside the patterned regions seems to be present as well, similar to findings when using the direct-dipping hydrothermal synthesis method.

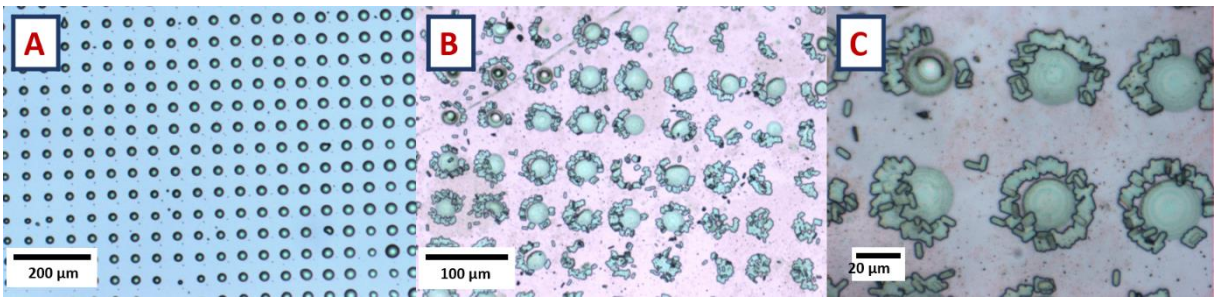

Figure 31: Optical micrograph of a spin-coated film (Si/Al=∞) on a SiO_2 coated Si wafer before hydrothermal step (A) and after 3 d at 423K with 200 µl H_2O.

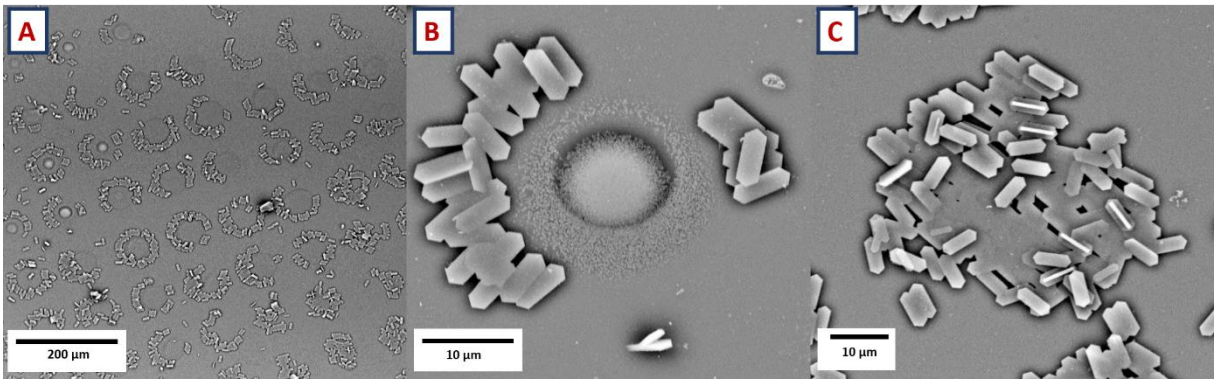

Figure 32: SEM image of a spin-coated film (Si/Al=∞) on a SiO_2 coated Si wafer after 3 d at 423 K with 200 µl H_2O.

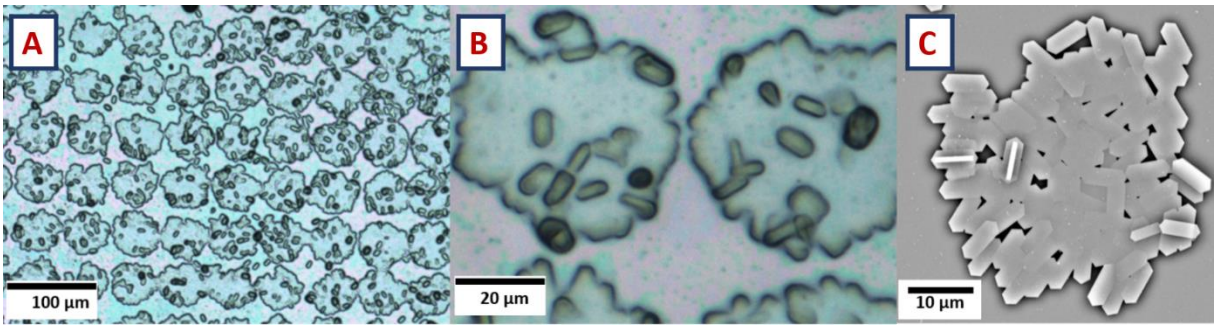

Figure 33: SEM image of a spin-coated film (Si/Al=∞) on a SiO_2 coated Si wafer after 3 d at 423 K with 200 µl H_2O.

In order to reduce the crystallization growth and random nucleation outside the patterned regions, the amount of water has been altered in the hydrothermal step. The hydrothermal step has been inspired on research performed by Wee et al [61] which use similar steam-assisted crystallization techniques for the synthesis silicalite-1 thin films. Figure 34 shows optical images and SEM image after a hydrothermal step using 20 µl water. A very thin layer of material is left and crystallization does not appear to have taken place. Upon increasing the amount of water to 40 µl (figure 35), crystalline phases are starting to form exclusively on the patterned regions.

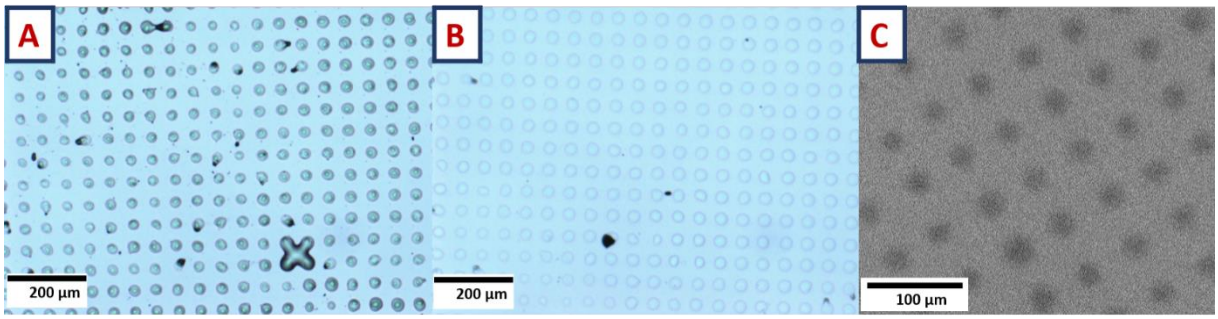

Figure 34: Optical micrograph of a spin-coated film (Si/Al=∞) on a SiO_2 coated Si wafer before hydrothermal step (A) and after 3 d at 423K with 200 µl H_2O (B) & SEM image after hydrothermal step (C). Diluted twice with ethanol.

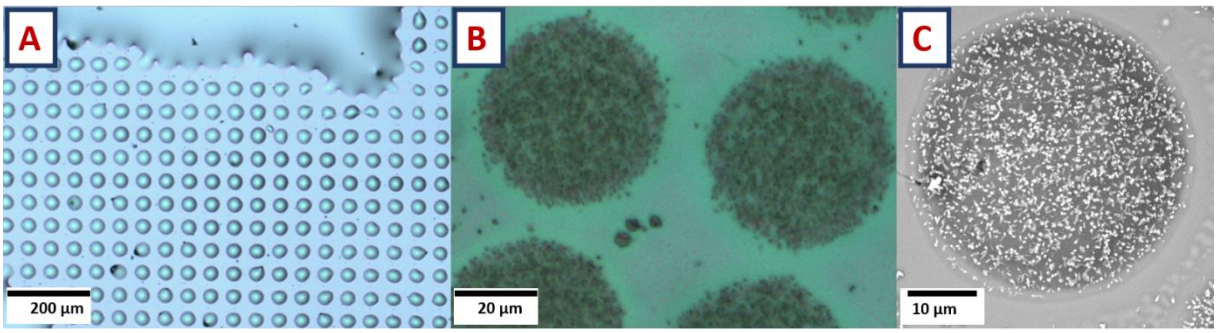

Figure 35: Optical micrograph of a spin-coated film (Si/Al=20) on a SiO_2 coated Si wafer before hydrothermal step (A) and after 3 d at 423K with 40 µl H_2O (B) & SEM image after hydrothermal step (C). Diluted twice with iso-propanol.

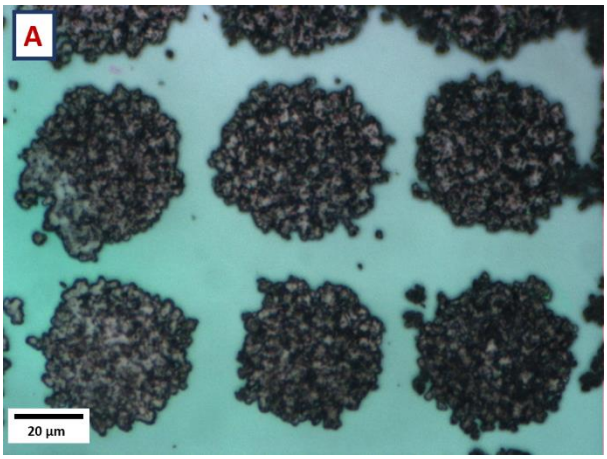

Figure 35: Optical micrograph of a spin-coated film (Si/Al= 160) on a SiO_2 coated Si wafer after 3 d at 493 K with 100 µl H_2O. Diluted twice with iso-propanol

With addition of 40 µl of H_2O during the hydrothermal step (figure 35), crystallization was incomplete and thus a spin-coated micropatterned film has been converted to crystalline material using 100 µl of H_2O (figure 36). The optical micrograph suggests that further crystallization had taken place and thus 100 µl of H_2O was used for other samples as well.

4.3.2 Influence of type of alcohol on zeolite micropattern formation

As described in section 2.2.1, spin-coating of a (colloidal) solution involves the evaporation of solvent during spinning of the substrate resulting in a layer of reaction precursor left behind**.** Ethanol plays a role in dissolving the silica source TEOS and water plays an important role of the subsequent hydrolysis of the silica species. In order to facilitate the spin-coating process and increase quality of micropatterning, alcohol species have been added to the reaction solution. The low viscosity of alcohols ensure good spreading of the solution over the substrate. Additionally, alcohols are able to influence the crystallization properties which allows for additional control over its morphology, orientation and thickness of the micropatterned films. [61]

-Ethanol, methanol and iso-propanol have been used to dilute the reaction solution.

The solutions have been twice, thrice and four times diluted with the alcohols. This decrease in viscosity has led to better spreading during spin-coating which resulted in a decreased rotation speed (2800 rpm for 30s). In general, higher rotation speeds lead to thinner films which leads to less zeolite material in each island. Since as much zeolite material as possible is desired, the solutions have been diluted the fewest amount of times, so twice. To increase proper spreading of the species, an acceleration of 100rpm/s has been used. A downside of the addition of alcohols to the solution gel is the decrease of concentration of silica and alumina species in the islands which means that fewer building blocks of zeolite crystals are available.

4.3.3 Spin-coating of neutral solution

While exploring the influence of the amount of water in the hydrothermal step, aluminium has been introduced into the precursor solution. As mentioned before, the presence of aluminate species influences the crystallization process of zeolite material considerably. [17,34,67] However, another important feature of a micropatterned model system which has

been investigated is its reproducibility and the control over the composition of the different islands of zeolite material. This prerequisite has given rise to an issue of practical nature which is the distribution of Al in the spin-coated patterns. Previously used aluminium sources, like $NaAlO_2$, are soluble in aqueous acidic media but not under basic conditions. At high pH, aluminium species tend to form which precipitate, such as $Al(OH)_3$, which would not be distributed equally amongst the spin-coated islands. Moreover, the addition of alcohols might improve the spreading during spin-coating but it decreases the solubility of aluminium sources. In a direct-dipping hydrothermal synthesis, all aluminium species are present in the synthesis gel and readily react while in the hydrothermal step after spin-coating, only a small amount of water is added to initiate crystallization. However, during the hydrothermal step, the elevated pressure and temperature can cause migration of species such as the water but also migration of alumina in vapor phase.[34] In order to minimize the effect of this migration, the synthesis must assure a homogeneous distribution of alumina species over the islands during spin-coating. For this reason, different aluminium sources have been explored as well as spin-coating of a neutral solution, using TPABr as template. This template still offers TPA^+ cations necessary for ZSM-5 synthesis while not affecting the pH.

Aluminium chloride hexahydrate ($AlCl_3.6\ H_2O$) has dissolved properly in the neutral solution and has consequently been used. Spin-coating of this solution has resulted in fewer islands than spin-coating the alkaline solution under the same spin-coating conditions but partially spin-coated samples have been synthesized and subjected to hydrothermal reaction.

As mentioned before, alkalinity plays a major role in ZSM-5 synthesis and since the spin-coated islands do not contain basic species such as OH^- anymore, this has to be introduced in the hydrothermal step. Therefore, bases like ammonia in water has been added in the autoclave to assist zeolite formation. Quantities of added base have been approximated on the amount of base available in the spin-coated patterns of basic precursor solution and quantities ranging from 10 µl to 500 µl ammonia solution have been added in the hydrothermal step.

Unfortunately, this hydrothermal step has not resulted in the formation of crystalline material yet. This could be caused by the difference in local alkalinity between micropatterns spin-coated with TPAOH and micropatterns spin-coated with TPABr and addition of a base source. Even though the pH has been approximated by adding an amount of base which theoretically results in similar concentrations, the alkaline species added in the hydrothermal step may not physically reach the substrate during hydrothermal step. Even if the basic solution reached the substrate as a vapour, it may have acted differently on molecular level. Moreover, the alkalinity of the synthesis solution leads to the formation of basic aluminate and silicate complexes during addition and stirring of the solution prior to spin-coating. Silicate is mostly present as $[SiO(OH)_3]^-$ or $[SiO_2(OH)_2]^{2-}$ and aluminate as $[Al(OH)_3OSi(OH)_3]^-$. [68] Addition of base after spin-coating during the hydrothermal step might cause different chemical behaviour and not result in the same species.

Spin-coating of an alkaline ZSM-5 precursor solution has led to well patterned zeolite crystals and spin-coating of neutral ZSM-5 precursor solution ensures presence of aluminium species and must be investigated further. However, both these methods lack an important characteristic of a micropatterned zeolite film model system which is the control over the composition of individual islands or patterns. This has led to the investigation of another method involving the manual microinjection of precursor solution onto a substrate.

4.4 Microinjection of a micropatterned zeolite model

Finally, a micropatterned zeolite thin film model system has been designed involving the microinjection of an alkaline and neutral synthesis solution onto a substrate followed by hydrothermal steaming to initiate zeolite crystallization. A number of influencing parameters have been investigated including the preparation of the substrate as well as the composition of the synthesis solution.

In the microinjection synthesis method, the zeolite precursor is manually applied onto the substrate using a microneedle. For practical reasons, this method has been realised using transparent substrates such as borosilicate and calcium fluoride. An additional benefit of a model system built on these substrates is the ability to utilize transmissive analysis techniques such as infrared spectroscopy and UV-VIS spectroscopy.

Figure 36 shows the optical micrograph of a microinjected model system using a siliceous alkaline precursor solution after a hydrothermal step consisting of 3 days at 423 K with addition of 100 µl water. The solution has been diluted 4 times with a stock of 35wt% EtOH in H_2O to ensure prevent clogging of the microneedle while providing the required concentration of water for crystallization. The optical image shows no observable zeolite crystals which might be caused by dilution lowering the concentration of zeolite precursors too much, filtration of essential components or due to substrate surface chemistry. Silicon based substrates offer silica species which take place in the crystallization reaction.

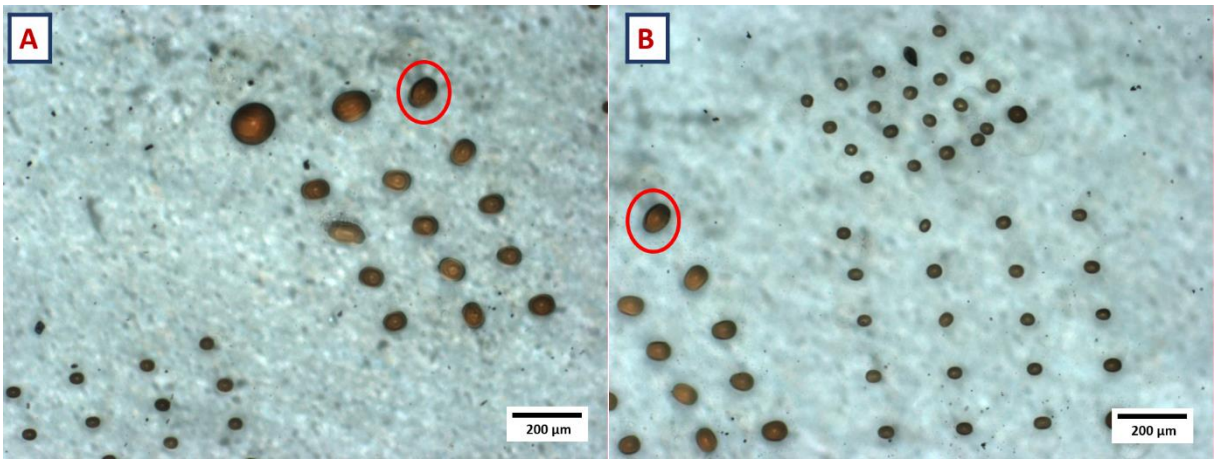

Figure 36: Optical micrograph of a microinjected zeolite model system (Si/Al=∞) on a borosilicate wafer after 3 d at 423 K with 100 µl H_2O. Diluted four times with EtOH.

The substrate has been manually micropatterned resulting in different areas of zeolite precursor material with tuneable size. Additionally, the position on the wafer of each area of islands is tuneable, the red circled island in figure 36A & B is the same island and shows the tunability and freedom of microinjection. A noticeable downside is the inconsistency of human labour which has led to different sized and shaped regions of zeolite material. However, this can be mechanized or solved by patterning the substrate beforehand, as has been done for the other methods used.

The influence of the preparation of borosilicate samples has been explored by applying different preparation procedures. In the first procedure, the substrate is cleaned of organic impurities through ultrasonication in a bath of water, ethanol and acetone. When analysing the resulting model system (figure 36) using AFM, it became apparent that the islands

were adsorbed to the surface rather than covalently bound since movement among the surface was observed. This was concluded by visual movement of the islands when touched by the AFM tip, as observed through the optical microscope of the AFM. In AFM, a probe is moved up and down the patterned island in order to measure i.a. its height, which pushed the island along the substrate surface.

Figure 37 shows an optical image of a borosilicate wafer microinjected with different zeolite precursor solutions in the same frame of measurement. Islands in region A have a silica to alumina ratio of Si/Al=∞ & for the islands in region B, Si/Al=20. The main advantage of this method, which is its high control over the composition of islands, has become clear. Further crystallization will lead to a micropatterned zeolite thin film model system which can be applied for testing the effect of one specific parameter, for example the Si/Al ratio of the zeolite, during catalytic reactions.

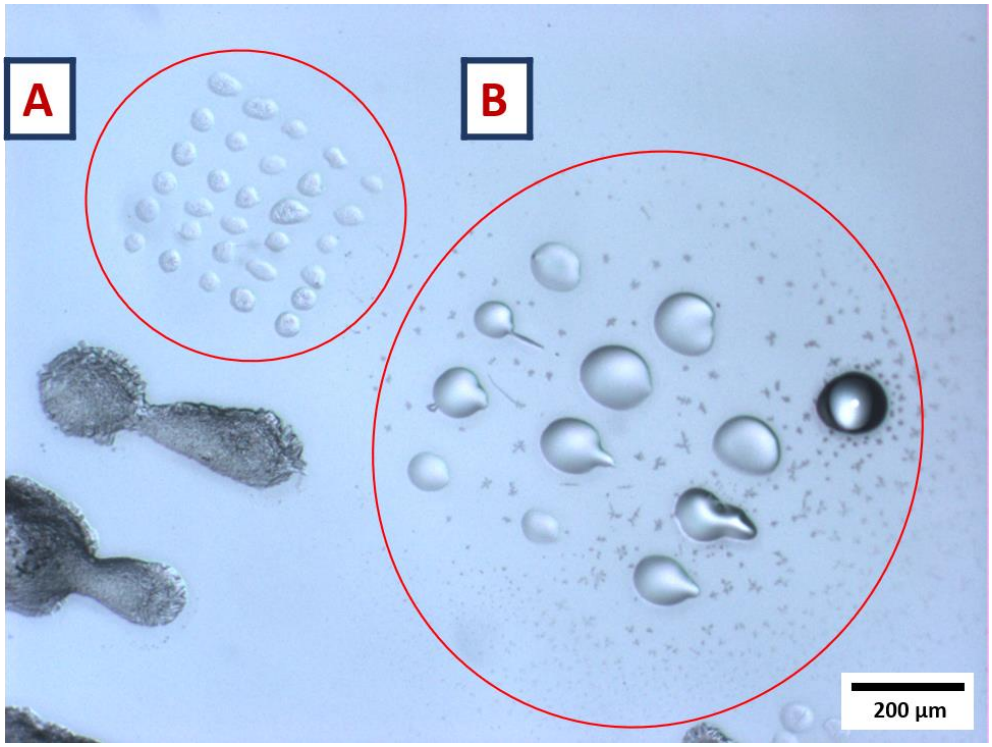

Figure 37: Optical micrograph of a microinjected zeolite model system on a borosilicate wafer with tunable Si/Al ratios on the same substrate. $Si/Al_{region\ A} = \infty$ & $Si/Al_{region\ B} = 20$. Diluted twice with EtOH.

In order to fix the issue of the zeolite precursor not covalently bonding to the surface, the substrate has been hydroxylated using a mixture of water, hydrogen peroxide and ammonia, next to the conventional cleaning method. This has resulted in better bonding to the surface although this high affinity with the substrate has resulted in a low contact angle which consecutively led to flattening of the islands. Furthermore, upon microinjection of diluted, volatile solutions, rapid evaporation of the solvent led to irregular non-circular shapes as well as sizes when using fully hydroxylated surfaces.

The irregularity and non-homogeneity of the model system has been solved by preparing the substrate in the same manner as for other methods; micropatterning alternating regions of hydrophobic and hydrophilic surface groups.

Similar to the spin-coating of ZSM-5 precursor solution, the composition of the islands before the hydrothermal step is important including the concentration of aluminium in the islands. Therefore, a neutral zeolite precursor solution has been microinjected containing template TPABr and $AlCl_3.6\ H_2O$ as alumina source. Additionally, undissolved alumina species could clog the microneedle or be filtered out so proper dissolving is important. Figure 38 shows three regions of the same borosilicate substrate microinjected with different precursor solution of different Si/Al ratios. For practical regions, the regions of different precursor solution are positioned a few millimetres apart but this can be altered so that islands of different compositions are visible in the same measuring frame.

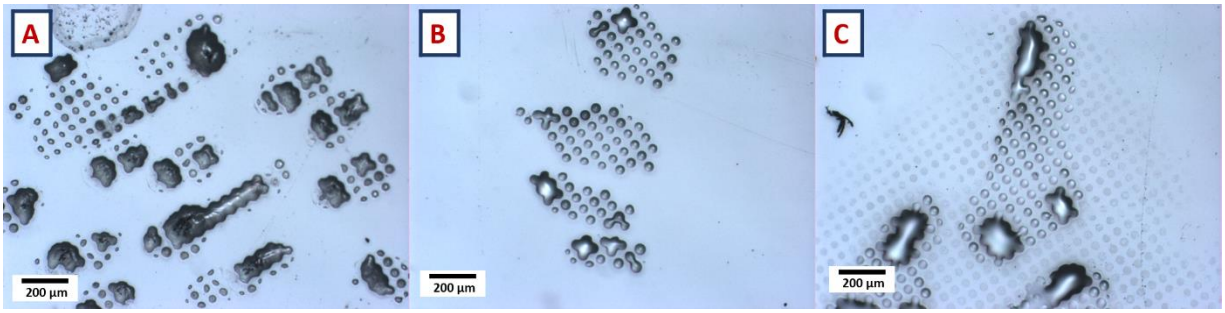

Figure 38: Optical micrograph of a microinjected zeolite model system on the same borosilicate wafer containing different compositions. A) Si/Al= ∞, b) Si/Al= 160, c) Si/Al= 20. Diluted twice with ethanol.

Further hydrothermal synthesis involving the addition of a base source in the autoclave can result in zeolite material.

4.5 X-Ray Diffraction characterization

X-Ray diffraction has been used to investigate the crystallinity of the synthesized model system as well as the presence of zeolite phase. Figure 39 shows the XRD pattern of micropatterned zeolite using different synthesis methods without incorporation of aluminium (Si/Al=0). This figure illustrates that the fabricated micropatterned thin films are crystalline which is characterized by the sharp peak present. Crystalline material has been synthesized using direct-dipping hydrothermal synthesis on a SiO_2 wafer (24 h, 423 K, sample from figure 24) as well as on a Si_3N_4 wafer (12 h, 393 K). Moreover, spin-coating of zeolite precursor followed by hydrothermal steaming has resulted in crystalline peaks (spin-coating, 3 d, 423 K, sample from figure 31 & figure 32). Figure 40 shows a better overview of the peaks at higher 2θ values.

The peak at 2θ=38° is caused by the crystallinity of the background silicon based wafer, either uncoated Si, Si_3N_4 or SiO_2 coated. Additional peaks around 2θ= 10°, 2θ =21°, 2θ=31° and 2θ=42° are found for all three synthesis methods suggesting that the same periodic crystal was formed.

MFI structures exhibit peaks at 2θ=10° and 2θ=24° which roughly corresponds with the measured peaks at 2θ= 10° & 2θ =21°, indicating synthesis of MFI silicalite-1 zeolite. [69]

Figure 39: XRD micropatterned thin films
Si/Al=0

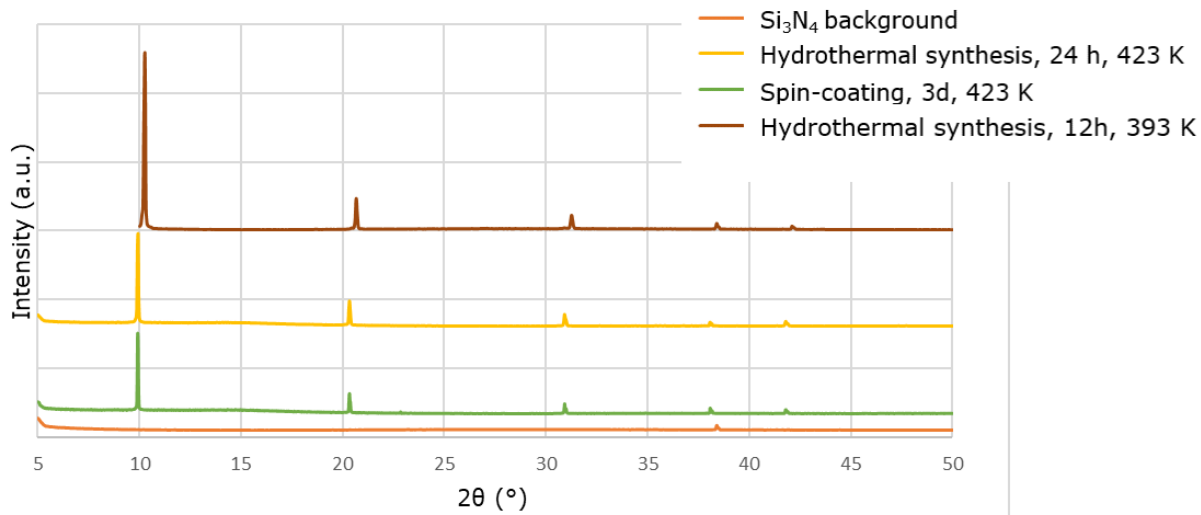

Figure 40: XRD micropatterned thin films
Si/Al=0

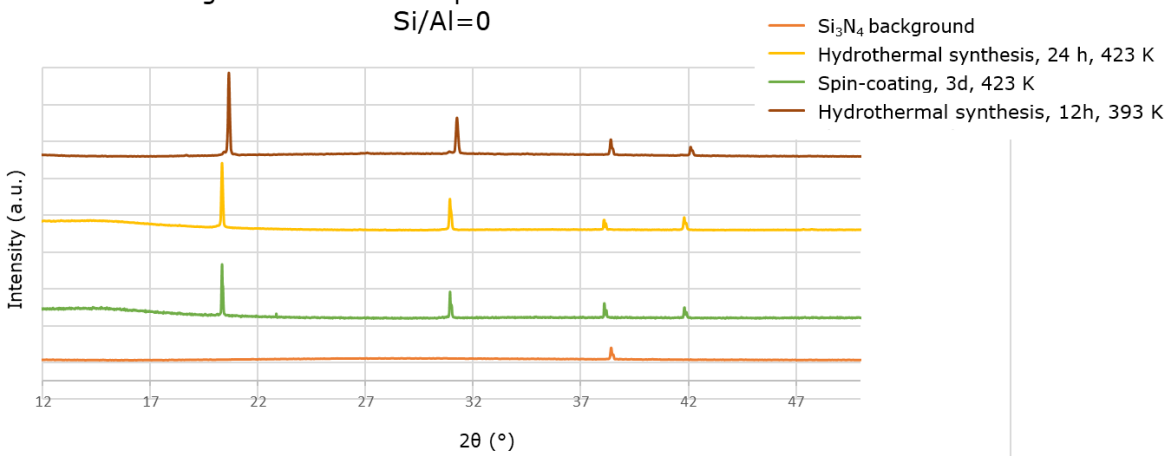

Figure 41: XRD micropatterned thin films
influence of Si/Al ratio

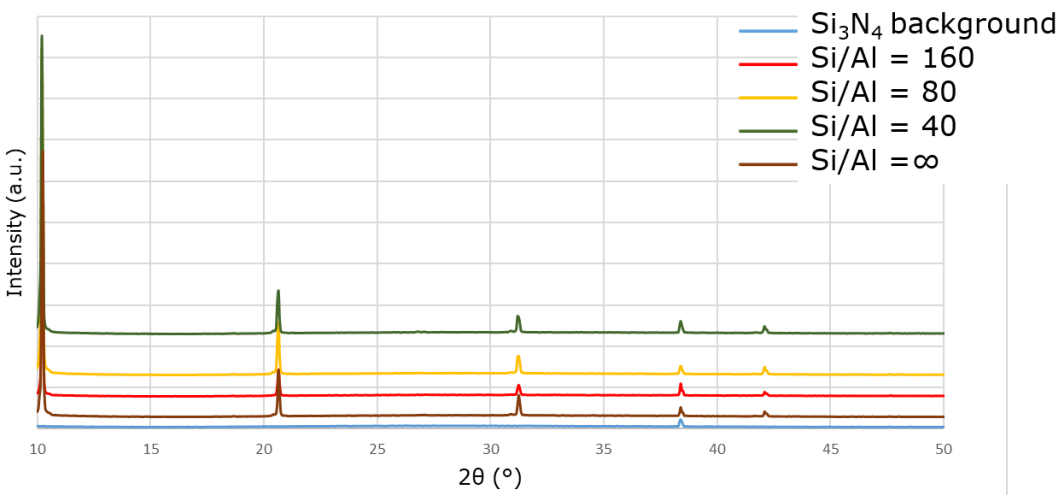

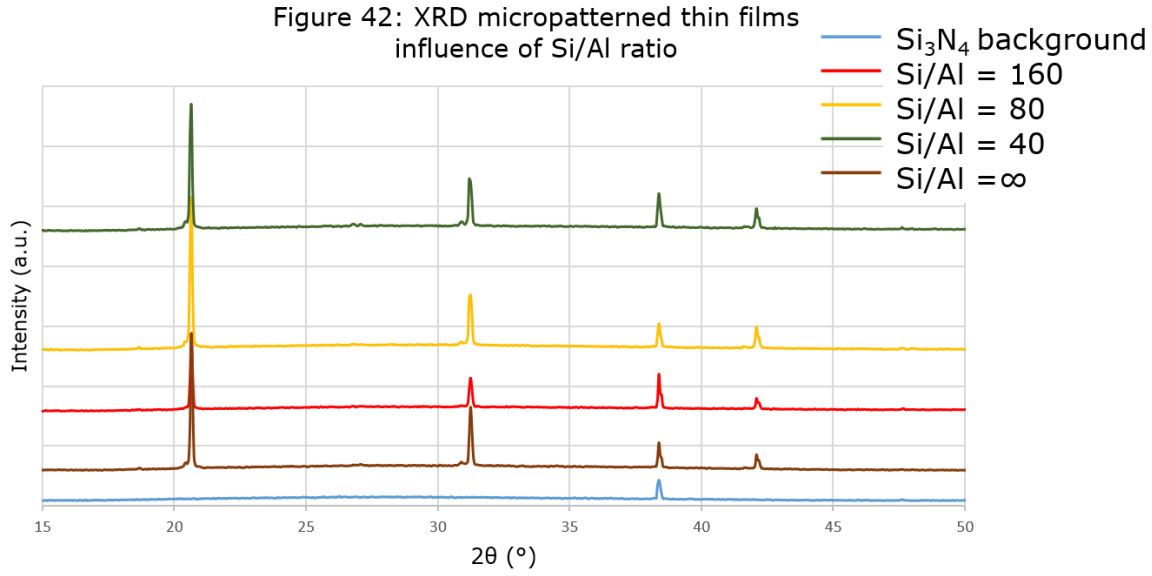

Figure 41 shows the XRD pattern of several micropatterned thin films synthesized using direct-dipping hydrothermal synthesis on Si_3N_4 wafers (12 h, 393 K). Different Si/Al ratios have been used in the synthesis and the difference in resulting crystallinity has been measured. Figure 42 shows a better overview of the peaks at higher 2θ values.

The Si_3N_4 background peak at 2θ=38° is shown in the XRD pattern and it has been found in all synthesized films. Moreover, a similar XRD pattern has been found when using different reaction conditions (figure 39). Additional peaks around 2θ= 10°, 2θ =21°, 2θ=31° and 2θ=42° are found for all three synthesis methods suggesting that the same periodic crystal was formed. There is no noticeable difference upon introducing aluminium in the synthesis gel which could be explained by noting that the aluminium might not have been incorporated correctly into the micropatterned zeolite or because the X-ray diffractograms of silicalite-1 and ZSM-5 are rather similar. [70]

It can be noted that the 2θ range of figure 41 & 42 was not large enough to measure all ZSM-5 reflections such as the <101> reflection at 2θ=7°.[71] In order to obtain more structural information from the XRD patterns, more measurements must be performed using differently prepared micropatterned model systems.

Chapter 5 – Conclusion

In this research, the development and fabrication of a micropatterned planar ZSM-5 model system has been investigated. Several synthesis approaches have been explored based on previous research regarding zeolite thin film model systems. Through analysis of the crystallinity and the quality of patterning using optical microscopy, SEM, AFM and XRD, initial findings have led to advances in the model design and fabrication.

Firstly, spin-coating of an acidic colloidal solution consisting of the precursor to fabricate SBA-15 has led to a better understanding of the sol-gel chemistry as well as the spin-coating process. For high amounts of added catalyst HCl (TEOS:HCl > 50), gelation of the sol occurs rapidly and the highest quality of patterning has been found after 5 min. till 30 min whereas for lower amounts (TEOS:HCl < 50) better micropatterning has been achieved after a gelation time of over 1 hour. Spin-coating settings have been explored and the best micropatterning has occurred at a rotation speed of 3000 rpm for 30 seconds. Spin-coating of an acidic colloidal has proven to be hard to predict and led to irreproducible results possibly caused by minor differences in colloidal composition, degree of gelation and spin-coating conditions. For this reason, combined with the increased labour demand of a multi-step process involving the recrystallization of SBA-15 to ZSM-5, other synthesis methods have been explored.

Secondly, direct-dipping hydrothermal synthesis of alkaline ZSM-5 synthesis gel has provided a facile method to fabricate a micropatterned model system. Investigation of the synthesis gel composition has resulted in excellent micropatterning at high Si/Al ratios and a decrease in quality of patterning when the aluminium content was increased. Hydrothermal synthesis of solutions containing Si/Al<40 has resulted in both overgrowth of crystals outside the patterned regions which can be attributed to the nature of aluminate to favour nucleation as well as a decrease of patterned islands which is due to its disrupting nature in zeolite crystallization. Moreover, the influence of the substrate has been investigated by preparing several silicon based substrates. It has been found that silicon substrates coated with Si_3N_4 or SiO_2 result in high quality of micropatterning while uncoated Si <100> results in degradation of the substrate which can be attributed to its high participation in the crystallization reaction.

Thirdly, spin-coating of ZSM-5 precursor solutions followed by steam-assisted hydrothermal step has led to zeolite micropatterns with high control over the quality of patterning. Previously acquired spin-coating knowledge has been applied and the spin-coating procedure has been adapted by addition of alcohols to the solution to facilitate homogenous spreading over the substrate. The influence of the addition of water in the hydrothermal step has been investigate; between 100 and 200 µl H_2O needs to be added to alkaline spin-coated wafers to favour complete crystallization. In order to facilitate solving of aluminium source and sequential incorporation of aluminium in the micropatterned islands, neutral ZSM-5 precursor solutions have been spin-coated. The amount of necessary added base in the hydrothermal step has been explored but has not resulted in a procedure leading to crystallization yet.

Finally, microinjection of ZSM-5 precursor solution onto transparent substrates followed by steam-assisted hydrothermal step has resulted in zeolite micropatterns with high control over the composition of individual islands. Preparation of the substrate involving micropatterning of alternating hydrophobic and hydrophilic areas has led to an ordered grid of circular microinjected islands (ø = 40µl) in exchange for loss over islands size and shape. Manual microinjection of patterns of multiple precursor solutions on the substrate has offered promising applications in high-throughput screening & catalytic testing. Microinjection of neutral ZSM-5 precursor solution followed by hydrothermal synthesis involving a base has not yet resulted in crystallization of zeolite material.

An overview of the different synthesis approaches for a micropatterned ZSM-5 thin film model system and their advantages and challenges shown in table 2.

Table 2: Overview of methods to synthesize micropatterned zeolite model system

Synthesis method	**Advantages**	**Drawbacks**
Spin-coating of acidic colloidal solution	High control over gelation precursor solution	Low reproducibility & multi-step synthesis
Direct-dipping hydrothermal synthesis	Facile synthesis	Random crystal growth
Spin-coating of an alkaline ZSM-5 precursor solution	High control over quality of micropatterning	Undissolved aluminium not incorporated in islands
Spin-coating of an alkaline ZSM-5 precursor solution	High control over quality of micropatterning	Precursor islands not converted into zeolite during hydrothermal synthesis
Microinjection of an alkaline & neutral ZSM-5 precursor solution	High control over composition individual islands on same model system	Labour-intensive method & islands not converted into zeolite during hydrothermal synthesis

Chapter 6 – Outlook

In this research, each approach of fabricating a model system has resulted in a better understanding of the chemical processes involved and more insight into the fabrication of the ideal micropatterned ZSM-5 thin film model system. However, this ideal model system has not been fabricated yet since the crystallization of microinjected micropatterns of neutral ZSM-5 precursor solution into ZSM-5 has not been realized nor optimised yet. Further experiments using different bases or different quantities may provide insight into the feasibility of this method.

Besides the characterization techniques which have been used, there are a number of additional techniques that could validate the synthesis of zeolite material and measure its composition. To start with, the aluminium content of the zeolite material can be measured through ammonia temperature programmed desorption (NH_3-TPD). This technique is widely used to characterize and measure the quantity of acid sites on oxide surfaces, like zeolites. Since the density of Brønsted acid site corresponds to the framework aluminium content, its incorporation in the micropatterned zeolite films can be validated. [72]

Additionally, the aluminium content can be measured through solid state nuclear magnetic resonance (^{27}Al-MAS-NMR). This technique measures the resonance caused by anisotropic interactions arising from the presence of aluminium nuclei. As a result, the local structure and the coordination of the aluminium species can be measured [73].

Another technique which can be used to measure the presence of aluminium in the synthesized zeolite species is through energy-dispersive spectroscopy (EDS). In EDS, excitation of the zeolite material results in electromagnetic emission which is unique for specific elements. EDS measurements of the synthesized model systems can provide a quick test of the presence and distribution of aluminium[74].

Not only can the aluminium source be varied but also the silica source leading to different zeolite characteristics. Even though TEOS has been widely researched, alternatives can be used in ZSM-5 synthesis. For example, the use of silica derived from low-grade industrial-processes as flotation tailings.

Next to alternative characterization techniques that could elucidate on the chemical composition of the synthesized micropatterned zeolite thin films, information can be gathered through catalytic testing of the model system. Since future applications of the zeolite films involve catalysis of several industrial processes, the presence of ZSM-5 can be tested by catalytic conversion such as methanol-to-olefins. An MTO set-up can be used with online mass spectrometer and operando UV-VIS measurements to measure the formed products during the reaction. Initial experiments have not resulted in an indication of the presence of coke-species which could mean that the conversion is not occurring or very slowly. This could potentially be caused by incorrect activation of the micropatterned zeolite thin film through incomplete ion-exchange of Na-ZSM-5 to NH_4-ZSM-5 or subsequent conversion to H-ZSM-5.

Another promising experiment to test the catalytic activity of ZSM-5 is the oligomerization of styrene[75]. During this reaction, dimeric and trimeric oligomers are formed which exhibit luminescent activity. These oligomers exhibit infrared activity, absorption and fluorescence which can be measured using infrared spectroscopy, UV-VIS-absorption spectroscopy and

confocal fluorescence microscopy. Confocal fluorescence microscopy measurements of the oligomerization of 4-fluorostyrene exhibit strong emission characteristic peaks which could be used to test the activity of the synthesized zeolite.[76] Initial analysis shows promising results indicating catalytic activity on a few islands of the micropatterned zeolite thin film model synthesized with direct-dipping hydrothermal synthesis (Figure 43). More research is required to improve mapping of catalytic activity by correcting for the background laser signal as well as measuring fluorescence at different focal planes.

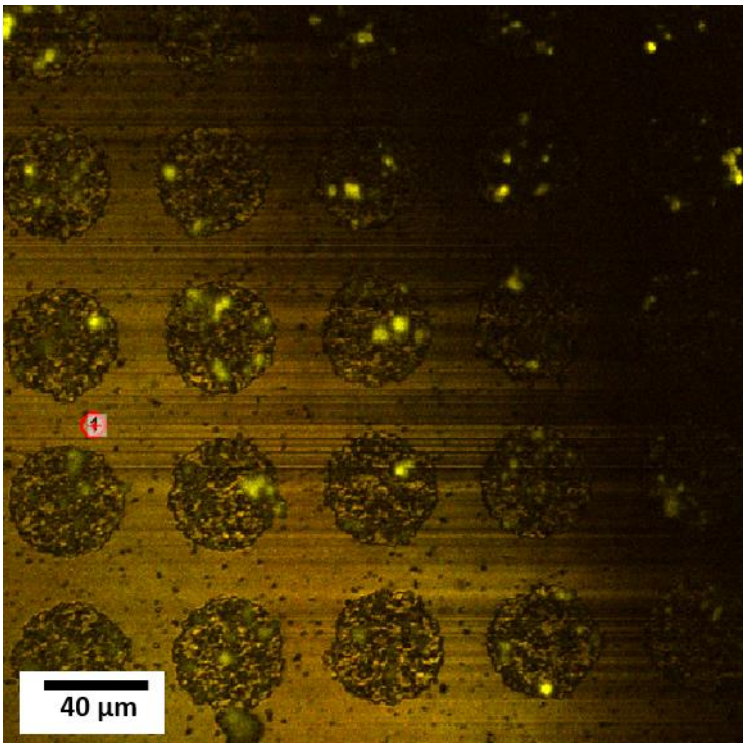

Figure 43: CFM image of a zeolite model system on a Si_3N_4 coated Si wafer after 2 h of oligomerization of 4-fluorostyrene at 423 K. Synthesized via direct-dipping hydrothermal synthesis. (12 h, 393 K, Si/Al= 200)

The oligomerization of 4-fluorostyrene can also be examined using UV-VIS-absorption spectroscopy, which is used to monitor the formation of carbocationic reaction intermediates.[77] This reaction can be monitored both in situ and ex situ using UV-VIS spectroscopy and provides information of the Brønsted acidity of the synthesised zeolite which correlates with the activity. Furthermore, analysis of the formed products provides information on the spatial morphology and microporous structure of the zeolite.

Another technique which can be used to measure the catalytic activity of the synthesized micropatterned zeolite films for the oligomerization of 4-fluorostyrene is infrared spectroscopy.[75] Comparison of IR spectra on zeolite islands, wafer background and zeolite which has remained unexposed to 4-fluorostyrene can be used to test the activity of the Additionally, IR mapping can provide an overview of the activity of the micropatterned zeolite film which will be valuable in high-throughput screening tests, especially when the micropatterned film has been synthesized using the microinjection method.

Finally, investigation of thin film zeolite model systems can provide elucidation on the limitations and observations of micropatterned thin film models. When similar colloidal solutions and synthesis gels are used on substrates which were not micropatterned before reaction, the difference between a homogeneous film and individual micropatterned islands can be measured in terms of morphology, thickness, catalytic activity and more.

Chapter 7 – Acknowledgements

During the course of this project, I have learned a lot regarding synthesis and characterization techniques as well as the fundamentals of performing research and the tasks and responsibilities which are a part of it.

I would like to thank the following people

Koen Bossers & Laurens Mandemaker for their guidance and sharing some of their inexhaustible wisdom with me, both in academia and in personal life. I would like to thank them in particular for their understanding and genuineness regarding a delay involving my literature review.

Prof. Bert Weckhuysen for agreeing to be my first examiner & welcoming me in the ICC group.

Dr. Florian Meirer for agreeing to be my second examiner & assisting me in the early stages of my project.

Yuanshuai Liu for assisting me in model synthesis and sharing his patterning knowledge

Nikos Nikolopoulus, Donglong Fu & other fellow ICC members for their assistance and the fun, social activities.

Chapter 8 – Bibliography

(1) Sarkodie, S. A.; Strezov, V. Effect of Foreign Direct Investments, Economic Development and Energy Consumption on Greenhouse Gas Emissions in Developing Countries. *Sci. Total Environ.* **2019**, *646*, 862–871.

(2) Martins, F.; Felgueiras, C.; Smitkova, M.; Caetano, N. Analysis of Fossil Fuel Energy Consumption and Environmental Impacts in European Countries. *Energies* **2019**, *12* (6), 964.

(3) Weitemeyer, S.; Kleinhans, D.; Vogt, T.; Agert, C. Integration of Renewable Energy Sources in Future Power Systems: The Role of Storage. *Renew. Energy* **2015**, *75*, 14–20.

(4) Hagen Jens. *Industrial Catalysis: A Practical Approach 3rd Ed - Jens Hagen (Wiley, 2015)*; **2015**. pp 1-4

(5) Thomas, S. J. M. The Advantages of Exploring the Interface Between Heterogeneous and Homogeneous Catalysis. *ChemCatChem* **2010**, *2* (2), 127–132.

(6) Jiang, N.; Shang, R.; Heijman, S. G. J.; Rietveld, L. C. High-Silica Zeolites for Adsorption of Organic Micro-Pollutants in Water Treatment: A Review. **2018**.

(7) Mozgawa, W.; Król, M.; Barczyk, K. FT-IR Studies of Zeolites from Different Structural Groups. *Chemik* **2011**, *65* (7), 671–674.

(8) Vyas, R. K.; Kumar, S. *Determination of Micropore Volume and Surface Area of Zeolite Molecular Sieves by D-R and D-A Equations: A Comparative Study*; **2004**; Vol. 11.

(9) Cejka, J.; van Bekkum, H.; Corma, A.; Schueth, F. *Introduction to Zeolite Molecular Sieves - Jiri Cejka, Herman van Bekkum, A. Corma, F. Schueth - Google Boeken*; **2007**. pp 56-57

(10) Csicsery, S. M. Shape-Selective Catalysis in Zeolites. *Zeolites*. Elsevier July 1, **1984**, pp 202–213.

(11) Munthali, M. W.; Elsheikh, M. A.; Johan, E.; Matsue, N. Proton Adsorption Selectivity of Zeolites in Aqueous Media: Effect of Si/Al Ratio of Zeolites. *Molecules* **2014**, *19* (12), 20468–20481.

(12) Yilmaz, B.; Müller, U. Catalytic Applications of Zeolites in Chemical Industry. In *Topics in Catalysis*; Springer, **2009**; Vol. 52, pp 888–895.

(13) Komvokis, V.; Tan, L. X. L.; Clough, M.; Pan, S. S.; Yilmaz, B. Zeolites in Fluid Catalytic Cracking (FCC). In *Zeolites in Sustainable Chemistry: Synthesis, Characterization and Catalytic Applications*; Springer Berlin Heidelberg, **2015**; pp 271–297.

(14) Daramola, M. O.; Aransiola, E. F.; Ojumu, T. V. Potential Applications of Zeolite Membranes in Reaction Coupling Separation Processes. *Materials (Basel).* **2012**, *5* (11), 2101–2136.

(15) Liu, Y. A.; Chang, A.-F.; Kiran, P. *Petroleum Refinery Process Modeling - Integrated Optimization Tools and Applications*; **2018**. pp240-242

(16) Kurdak, C. ¸; Kim, J.; Farina, L. A.; Lewis, K. M.; Bai, X.; Rowe, M. P.; Matzger, A. J. *Au Nanoparticle Clusters: A New System to Model Hopping Conduction*.

(17) Fu, D.; Schmidt, J. E.; Ristanović, Z.; Chowdhury, A. D.; Meirer, F.; Weckhuysen, B. M. Highly Oriented Growth of Catalytically Active Zeolite ZSM-5 Films with a Broad Range of Si/Al Ratios. *Angew. Chemie Int. Ed.* **2017**, *56* (37), 11217–11221.

(18) Mandemaker, L. D. B.; Filez, M.; Delen, G.; Tan, H.; Zhang, X.; Lohse, D.; Weckhuysen, B. M. Time-Resolved In Situ Liquid-Phase Atomic Force Microscopy and Infrared Nanospectroscopy during the Formation of Metal−Organic Framework Thin Films. *J. Phys.*

Chem. Lett **2018**, *9*, 1838–1844.

(19) Yeo, B.-S.; Amstad, E.; Schmid, T.; Stadler, J.; Zenobi, R. Nanoscale Probing of a Polymer-Blend Thin Film with Tip-Enhanced Raman Spectroscopy. *Small* **2009**, *5* (8), 952–960.

(20) Metzger, T. H.; Mintova, S.; Bein, T. Nanoscale Crystal Orientation in Silicalite-1 Films Studied by Grazing Incidence X-Ray Diffraction. *Microporous Mesoporous Mater.* **2001**, *43* (2), 191–200.

(21) Fu, D.; Park, K.; Delen, G.; Attila, Ö.; Meirer, F.; Nowak, D.; Park, S.; Schmidt, J. E.; Weckhuysen, B. M. Nanoscale Infrared Imaging of Zeolites Using Photoinduced Force Microscopy. *Chem. Commun.* **2017**, *53* (97), 13012–13014.

(22) Li, Y.; Li, L.; Yu, J. Applications of Zeolites in Sustainable Chemistry. *Chem*. Elsevier Inc December 14, **2017**, pp 928–949.

(23) Lew, C. M.; Cai, R.; Yan, Y. Zeolite Thin Films: From Computer Chips to Space Stations. *Acc. Chem. Res.* **2010**, *43* (2), 210–219.

(24) Wen, Q.; Di, J.; Jiang, L.; Yu, J.; Xu, R. Zeolite-Coated Mesh Film for Efficient Oil-Water Separation. *Chem. Sci.* **2013**, *4* (2), 591–595.

(25) Fu, T.; Zhou, H.; Li, Z. Effect of Particle Morphology for ZSM-5 Zeolite on the Catalytic Conversion of Methanol to Gasoline-Range Hydrocarbons. *Catal. Letters* **2016**, *146* (10), 1973–1983.

(26) Ha, K.; Lee, Y. J.; Chun, Y. S.; Park, Y. S.; Lee, G. S.; Yoon, K. B. Photochemical Pattern Transfer and Patterning of Continuous Zeolite Films on Glass by Direct Dipping in Synthesis Gel. *Adv. Mater.* **2001**, *13* (8), 594–596.

(27) Bajorath, J. Integration of Virtual and High-Throughput Screening. *Nature Reviews Drug Discovery*. Nature Publishing Group November 2002, pp 882–894.

(28) Shaughnessy, K. H.; Kim, P.; Hartwig, J. F. A Fluorescence-Based Assay for High-Throughput Screening of Coupling Reactions. Application to Heck Chemistry. *J. Am. Chem. Soc.* **1999**, *121* (10), 2123–2132.

(29) Zeng, Y.; Hua, Z.; Tian, X.; Li, X.; Qiu, Z.; Zhang, C.; Wang, M.; Li, E. ping. Selective Detection of Methanol by Zeolite/Pd-WO3 Gas Sensors. *Sensors Actuators, B Chem.* **2018**, *273*, 1291–1299.

(30) Liu, X.; Shen, Y.; Yang, R.; Zou, S.; Ji, X.; Shi, L.; Zhang, Y.; Liu, D.; Xiao, L.; Zheng, X.; et al. Inkjet Printing Assisted Synthesis of Multicomponent Mesoporous Metal Oxides for Ultrafast Catalyst Exploration. *Nano Lett* **2012**, *12*, 14.

(31) Moshoeshoe, M.; Silas Nadiye-Tabbiruka, M.; Obuseng, V. A Review of the Chemistry, Structure, Properties and Applications of Zeolites. *Am. J. Mater. Sci.* **2017**, *2017* (5), 196–221.

(32) De, S.; Dutta, S.; Saha, B. Catalysis Science & Technology MINIREVIEW Critical Design of Heterogeneous Catalysts for Biomass Valorization: Current Thrust and Emerging Prospects. *Cite this Catal. Sci. Technol* **2014**, *6*, 7364.

(33) Almutairi, S. M. T.; Mezari, B.; Filonenko, G. A.; Magusin, P. C. M. M.; Rigutto, M. S.; Pidko, E. A.; Hensen, E. J. M. Influence of Extraframework Aluminum on the Brønsted Acidity and Catalytic Reactivity of Faujasite Zeolite. *ChemCatChem* **2013**, *5* (2), 452–466.

(34) Li, T.; Krumeich, F.; Van Bokhoven, J. A.; Zurich, E.; Insitute, P. S.; Switzerland, V. Where Does the Zeolite ZSM-5 Nucleation and Growth Start? The Effect of Aluminum. **2019**.

(35) Grand, J.; Awala, H.; Mintova, S. Mechanism of Zeolites Crystal Growth: New Findings and Open Questions. *CrystEngComm* **2016**, *18* (5), 650–664.

(36) Schoeman, B. J. *Analysis of the Nucleation and Growth of TPA-Silicalite-1 at Elevated Temperatures with the Emphasis on Colloidal Stability1*; **1998**; Vol. 22.

(37) Nikolakis, V.; Kokkoli, E.; Tirrell, M.; Tsapatsis, M.; Vlachos, D. G. Zeolite Growth by Addition of Subcolloidal Particles: Modeling and Experimental Validation. **2000**.

(38) Couture, G.; Alaaeddine, A.; Boschet, F.; Ameduri, B. Polymeric Materials as Anion-Exchange Membranes for Alkaline Fuel Cells. *Progress in Polymer Science (Oxford)*. Pergamon November 1, **2011**, pp 1521–1557.

(39) C. Jeffrey Brinker, G. W. S. Sol-Gel Science: The Physics and Chemistry of Sol-Gel Processing. The Physics and Chemistry of Sol-Gel. **2013,** pp1 31-134

(40) Lofgreen, J. E.; Ozin, G. A. Controlling Morphology and Porosity to Improve Performance of Molecularly Imprinted Sol-Gel Silica. *Chemical Society Reviews*. Royal Society of Chemistry February 7, **2014**, pp 911–933.

(41) Colleoni, C.; Esposito, S.; Grasso, R.; Gulino, M.; Musumeci, F.; Romeli, D.; Rosace, G.; Salesi, G.; Scordino, A. Delayed Luminescence Induced by Complex Domains in Water and in TEOS Aqueous Solutions. *Phys. Chem. Chem. Phys.* **2016**, *18* (2), 772–780.

(42) Comite, A. Preparation of Silica Membranes by Sol-Gel Method. In *Current Trends and Future Developments on (Bio-) Membranes: Silica Membranes: Preparation, Modelling, Application, and Commercialization*; Elsevier Inc., **2017**; pp 3–23.

(43) Rahmat, N.; Abdullah, A. Z.; Mohamed, A. R. A Review: Mesoporous Santa Barbara Amorphous-15, Types, Synthesis and Its Applications towards Biorefinery Production. *American Journal of Applied Sciences*. Science Publications **2010**, pp 1579–1586.

(44) Chaudhary, V.; Sharma, S. An Overview of Ordered Mesoporous Material SBA-15: Synthesis, Functionalization and Application in Oxidation Reactions. *J. Porous Mater.* **2017**, *24* (3), 741–749.

(45) Zeleňáková, A.; Hrubovčák, pavol; Kapusta, ondrej; Kučerka, norbert; Kuklin, A.; Ivankov, O.; Zeleňák, V. Size and Distribution of the Iron Oxide Nanoparticles in SBA-15 Nanoporous Silica via SANS Study. *9*.

(46) Campos, A. A.; Dimitrov, L.; Da Silva, C. R.; Wallau, M.; Urquieta-González, E. A. Recrystallisation of Mesoporous SBA-15 into Microporous ZSM-5. **2006**.

(47) Kato, K.; Nakamura, H.; Yamauchi, Y.; Nakanishi, K.; Tomita, M. Preparation of Mesoporous Silica Thin Films by Photocalcination Method and Their Adsorption Abilities for Various Proteins. *Mater. Sci. Eng. C* **2014**, *40*, 42–48.

(48) Guhathakurta, S.; Subramanian, A. Effect of Hydrofluoric Acid in Oxidizing Acid Mixtures on the Hydroxylation of Silicon Surface. *J. Electrochem. Soc.* **2007**, *154* (11), P136.

(49) Bohling, C.; Sigmund, W. Self-Limitation of Native Oxides Explained. *Silicon* **2016**, *8* (3), 339–343.

(50) Poole, C. F. High-Performance Precoated Stationary Phases. In *Instrumental Thin-Layer Chromatography*; Elsevier Inc., **2015**; pp 31–51.

(51) McGovern, M. E.; Kallury, K. M. R.; Thompson, M. Role of Solvent on the Silanization of Glass with Octadecyltrichlorosilane. *Langmuir* **1994**, *10* (10), 3607–3614.

(52) Han, X.; Wang, L.; Li, J.; Zhan, X.; Chen, J.; Yang, J. Tuning the Hydrophobicity of ZSM-5 Zeolites by Surface Silanization Using Alkyltrichlorosilane. *Appl. Surf. Sci.* **2011**, *257* (22), 9525–9531.

(53) Vig, J. R. UV/Ozone Cleaning of Surfaces. In *Proceedings - The Electrochemical Society*; Publ by Electrochemical Soc Inc, **1990**; Vol. 90, pp 105–113.

(54) Sheffer, M.; Groysman, A.; Mandler, D. Electrodeposition of Sol-Gel Films on Al for Corrosion Protection. *Corros. Sci.* **2003**, *45* (12), 2893–2904.

(55) Momeni, M.; Golestani-Fard, F.; Saghafian, H.; Barati, N.; Khanahmadi, A. Development of Visible Light Activated TiO 2 Thin Films on Stainless Steel via Sol Spraying with Emphasis on

Microstructural Evolution and Photocatalytic Activity. *Appl. Surf. Sci.* **2015**, *357*, 1902–1910.

(56) Kakaei, K.; Esrafili, M. D.; Ehsani, A. Graphene and Anticorrosive Properties. In *Interface Science and Technology*; Elsevier B.V., 2019; Vol. 27, pp 303–337.

(57) Li, Q. Sol-Gel Coatings to Improve the Corrosion Resistance of Magnesium (Mg) Alloys. In *Corrosion Prevention of Magnesium Alloys: A volume in Woodhead Publishing Series in Metals and Surface Engineering*; Elsevier Ltd, 2013; pp 469–485.

(58) Lee, U. G.; Kim, W.-B.; Han, D. H.; Chung, H. S. A Modified Equation for Thickness of the Film Fabricated by Spin Coating. *Symmetry (Basel).* **2019**, *11* (9), 1183.

(59) Bachman, M. *RCA-2 Silicon Wafer Cleaning INRF Application Note Process Name: RCA02*; 2002.

(60) Huirache-Acuña, R.; Nava, R.; Peza-Ledesma, C.; Lara-Romero, J.; Alonso-Núez, G.; Pawelec, B.; Rivera-Muñoz, E. SBA-15 Mesoporous Silica as Catalytic Support for Hydrodesulfurization Catalysts—Review. *Materials (Basel).* **2013**, *6* (9), 4139–4167.

(61) Wee, L. H.; Tosheva, L.; Itani, L.; Valtchev, V.; Doyle, A. M. Steam-Assisted Synthesis of Zeolite Films from Spin-Coated Zeolite Precursor Coatings. **2008**.

(62) Nishi, K.; Thompson, R. W. Synthesis of Classical Zeolites. In *Handbook of Porous Solids*; Wiley-VCH Verlag GmbH: Weinheim, Germany, 2008; pp 736–814.

(63) Paper, C.; Moghimpour, P.; Petrochemical, B.; Industry, P. Effect of PH on the Synthesis of ZSM-5 Zeolite Using TEOS and Performance of H-ZSM-5 Catalyst in Propane Aromatization. **2015**, No. April 2016, 1–6.

(64) Burkett, S. L.; Davis, M. E. Mechanism of Structure Direction in the Synthesis of Si-ZSM-5 : An Investigation by Intermolecular 1H-29Si CP MAS NMR Mechanism of Structure Direction in the Synthesis of Si-ZSM-5 : An Investigation by Intermolecular 1H-29Si CP MAS NMR. *J. Phys. Chem.* **1994**, *98* (17), 4647–4653.

(65) Roeffaers, M. Heterogeneous Catalysis : A Fluorescence Microscopy. *PHD* **2008**.

(66) Lipin, Y.; Machevski, E. Protective Properties of Silicon Nitride, Deposited by Bias Reactive Sputtering. *Proceedings, Annu. Tech. Conf. - Soc. Vac. Coaters* **1999**, 133–135.

(67) Mohamed, R. M.; Fouad, O. A.; Ismail, A. A.; Ibrahim, I. A. Influence of Crystallization Times on the Synthesis of Nanosized ZSM-5. *Mater. Lett.* **2005**, *59* (27), 3441–3444.

(68) Lechert, H. The pH-value and its importance for the crystallization of zeolites http://www.iza-online.org/synthesis/VS_2ndEd/pH.htm (accessed Apr 16, 2020).

(69) Martins, L.; Peguin, R. P. S.; Urquieta-González, E. A. Cu and Co Exchanged ZSM-5 Zeolites - Activity towards NO Reduction and Hydrocarbon Oxidation. *Quim. Nova* **2006**, *29* (2), 223–229.

(70) Zhang, J.; Li, X.; Liu, J.; Wang, C. A Comparative Study of MFI Zeolite Derived from Different Silica Sources: Synthesis, Characterization and Catalytic Performance. *Catalysts* **2019**, *9* (1).

(71) Zampieri, A.; Dubbe, A.; Schwieger, W.; Avhale, A.; Moos, R. ZSM-5 Zeolite Films on Si Substrates Grown by in Situ Seeding and Secondary Crystal Growth and Application in an Electrochemical Hydrocarbon Gas Sensor. *Microporous Mesoporous Mater.* **2008**.

(72) Čejka, J.; Corma, A.; Zones, S. *Zeolites and Catalysis: Synthesis, Reactions and Applications*; 2010; Vol. 1–2. pp 498-499

(73) Sklenak, S.; Jirˇı´, J.; Jirˇı´deˇdeček, J.; Li, C.; Wichterlova´, B. W.; Ga´bova´, V.; Ga´bova´, G.; Sierka, M.; Sauer, J. Aluminium Siting in the ZSM-5 Framework by Combination of High Resolution 27 Al NMR and DFT/MM Calculationsw.

(74) Razavian, M.; Fatemi, S.; Komasi, M. Seed-Assisted OSDA-Free Synthesis of ZSM-5 Zeolite and Its Application in Dehydrogenation of Propane. **2015**.

(75) Stavitski, E.; Kox, M. H. F.; Weckhuysen, B. M. *An Eye on the inside of Zeolite Crystals in the Act: Studying Brønsted Acidity with in-Situ Micro-Spectroscopy*; Elsevier B.V., 2008; Vol. 174.

(76) Sprung, C.; Weckhuysen, B. M. Differences in the Location of Guest Molecules within Zeolite Pores as Revealed by Multilaser Excitation Confocal Fluorescence Microscopy: Which Molecule Is Where? *J. Am. Chem. Soc.* **2015**, *137* (5), 1916–1928.

(77) Buurmans, I. L. C.; Pidko, E. A.; de Groot, J. M.; Stavitski, E.; van Santen, R. A.; Weckhuysen, B. M. Styrene Oligomerization as a Molecular Probe Reaction for Zeolite Acidity: A UV-Vis Spectroscopy and DFT Study. *Phys. Chem. Chem. Phys.* **2010**, *12* (26), 7032–7040.

Chapter 9 – Appendices

9.1 Appendix A: Results Spin-coating of SBA-15 precursor under acidic conditions

The initial colloidal solution contains the molar ratio of TEOS:H_2O:EtOH:HCl:P123 = 1 : 15.1 : 38.1 : 0.16 : 0.01 . The composition of the colloidal solution has been altered by changing the water to ethanol ratio, the amount of catalytic HCl and the amount of organic template.

The water to ethanol ratio has been examined in order to change the viscosity of the colloidal solution and also influence its affinity to the wafer with as goal to successfully spin-coat a micropattern of SBA-15 precursor on the prepared substrate. The ratios that have been examined are shown in table 3. Bold marked numbers show ethanol/water ratios that have led to (partial) successfully spin-coated wafers.

Table 3: Ethanol / water molar ratio	
∞ (no H_2O)	**1.7**
3.8	**1.6**
3.2	1.0
2.6	**0.6**
2.5 (literature)	**0.3**

There is no trend in the ethanol to water ratio and the degree of spin-coating of the sample. This was mostly influenced by the other parameters such as the catalyst concentration and the gelation time.

Table 4: Ratio of HCl added / HCl added in literature	
0.4	**8.0**
1.0 (literature)	**12**
3.2	28
6.4	**32**

A trend has been found which states that the gelation rate increases upon increasing the catalyst concentration.

9.2 Appendix B: Influence preparation of substrate in direct-dipping hydrothermal synthesis

The hydroxylation step has been investigated by altering the H_2O:H_2O_2:NH_3 volume ratio and reaction duration and comparing the degree and quality of resulting micropatterned thin films in spin-coating and direct-dipping hydrothermal synthesis.

The following volume ratio of H_2O:H_2O_2:NH_3= 5:1:1 has been investigated for 20, 30 & 45 min and volume ratio H_2O:H_2O_2:NH_3= 0:1:1 for 10 minutes. No significant differences have been found.

Another step in the preparation of substrates which has been investigated is the application of an alkylsilane onto the hydroxylated surface under inert atmosphere. Octadecyl-trichlorosilane (ODTS) and octadecyl-trimethoxysilane (OTMS) have been investigated. Since OTMS is less reactive than ODTS, the solution has been refluxed to ensure formation of a monolayer onto the prepared substrate. No significant differences in patterning have been found between the two preparation methods.

9.3 Appendix C: AFM tip testing

AFM has been used to investigate the crystalline properties of the synthesized model systems including the island height, distribution and roughness as well as the morphology of the zeolite material including presence of porosity. Since AFM tips are able to analyse a surface with atomic scale precision, they are prone to contamination or deterioration. Because of the high strength and durability of zeolite phases, they are able to readily cause damage or contaminate the AFM tip during measurements.

In order to utilize the best AFM tip for the measurement of synthesized zeolite material, a variety of AFM tips have been tested on a crystalline micropattern. The following tips have been tested by measuring AFM in tapping mode of micropatterned zeolite model synthesized using the method of spin-coating an alkaline ZSM-5 precursor solution:

DP15, HA_NC side a & b & NSC_14

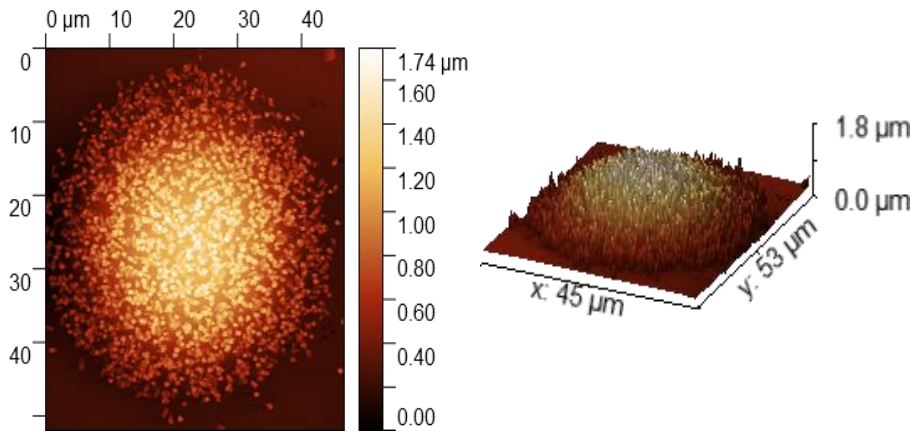

Figure 44: AFM images of a zeolite micropatterned film (Si/Al=20) synthesized using spin-coating of alkaline solution followed by hydrothermal step (3d, 423 K, 40µl H_2O, SiO_2 coated wafer using a DP15 tip.

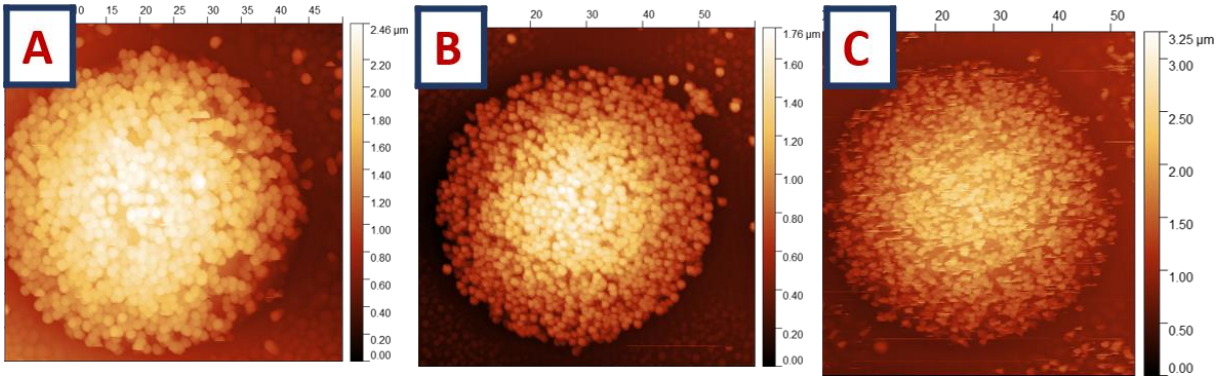

Figure 45: AFM images of zeolite micropattern using A) HA_NC side a tip, B) HA_NC side b, C) NSC_14

Figure 44 shows the optical image and AFM image of micropatterned zeolite islands synthesized using the spin-coating of an alkaline solution method followed by hydrothermal treatment (3d, 423 K, 100 µl H_2O). The AFM image shows a hemispherical island with small crystalline particles protruding from the surface.

The same sample (different areas) has been analysed with AFM using different tips or probes shown in figure 45. The resultant island height range from 1.76 µm to 3.25 µm which is feasible since the patterning is not equal for the entire surface the substrate. However, in figure 45, strangely shaped objects have been observed present on the entire surface. These artifacts have most likely been caused by a damage tip, as explained by figure 46.

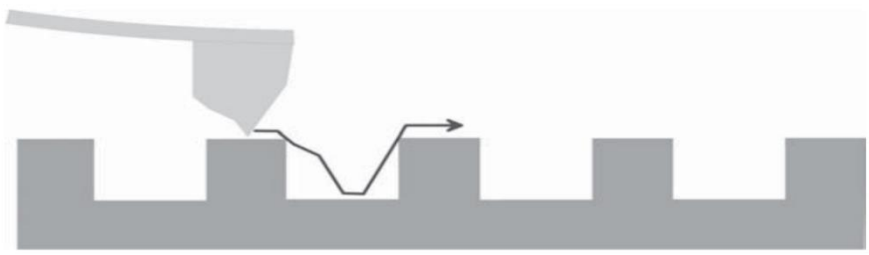

Figure 46: Schematic image of the signal of a damaged AFM tip scanning a surface

Even though the AFM tip DP15 appears to be the best fit to measure micropatterned zeolite thin film models, crashes of the tip have also occurred and careful handling is necessary for each tip.